THESIS FOR THE DEGREE OF DOCTOR OF PHILOSOPHY

Natural corrosion in reinforced concrete structures

Samanta Robuschi

CHALMERS
UNIVERSITY OF TECHNOLOGY

Department of Department of Architecture and Civil Engineering
Chalmers University of Technology
Gothenburg, Sweden, 2021

Natural corrosion in reinforced concrete structures

Samanta Robuschi

Technical Report No. 5014
ISSN 978-91-7905-547-9
This thesis has been prepared using LaTeX.

Department of Department of Architecture and Civil Engineering
Chalmers University of Technology
SE-412 96 Gothenburg, Sweden
Phone: +46 (0)31 772 1000
www.chalmers.se

Cover:
Representation of Gullspång bridge and overview of the different studies and experimental tests conducted in the thesis.

Printed by Chalmers Reproservice
Gothenburg, Sweden, December2021

To Felix, la mia persona preferita

Abstract

Among the treats to the durability of concrete structures, corrosion of the reinforcement bars is undoubtedly the most common one. Corrosion damages impair safety and durability of infrastructure, and assessment of the safety is challenging due to the complex nature of the corrosion process. Furthermore, research on the topic often requires adapting results from short-time laboratory tests, where corrosion of the reinforcement bars is induced using impressed current, to the reality of existing structures. The use of impressed current results in differences in type and distribution of corrosion products. Naturally corroded specimens are hence the necessary bridge between the knowledge acquired from artificially corroded specimens and the application to real structures. This works investigates the structural effects of natural, chloride-induced corrosion in reinforced concrete structures. Specifically, three research questions were investigated. First, the bond and anchorage of naturally corroded plain bars was studied using 3-point bending and pull-out tests. The tests were designed to be applied to specimens taken from a decommissioned bridge from the 1930s. The bond capacity of plain bars was observed to be significantly higher than in results obtained from laboratory tests on similar bars. Significant factors influencing the effect of corrosion damages on the bond were casting position and presence of stirrups. Finite element analyses were used to further investigate the bond-slip behaviour of the tested specimens. The results highlighted the effect of the loss of bond at yielding on the structural behaviour of the specimens. The second question looked into the characteristics of the corrosion products and the surrounding concrete; this is relevant to assess corrosion damages in existing structures. Neutron imaging and X-ray computed tomography were used to obtain qualitative and quantitative data on corrosion damages in a naturally corroded specimens, including iron to rust ratio. Comparison with an artificially corroded specimen showed differences in distribution of the corrosion products. Finally, possible correlations between transversal cracks and corrosion damages was investigated. A dataset was compiled from experiments available in literature. In the selected studies, corrosion of the steel reinforcement resulted from exposing laboratory specimens, pre-cracked in 3-point bending, to chloride environments. No clear correlation between surface crack width and corrosion characteristics was found, but corrosion pits were shown to likely appear in the proximity of transveral cracks. To conclude, this work highlights the complexity of the corrosion process and argues that a thorough understanding of the material and environmental characteristics influencing this process is necessary to properly assess existing structures. Tests on naturally corroded structures are a fundamental step towards acquiring this knowledge.

Keywords: Natural corrosion, reinforced concrete structures, plain bars, anchorage, neutron imaging, X-rays CT, pitting corrosion, chloride-induced corrosion.

Sammanfattning

Korroderande armering är den vanligaste skadetypen i armerad betong. Korrosionsskador försämrar säkerheten och förkortar livslängden hos betongkonstruktioner, och korrosionsprocessens komplexitet gör bedömningar av säkerheten utmanande. Detta beror delvis på svårigheterna i att tolka resultat från accelererade laboratorieförsök med pålagd spänning för att korta korrosionstiden, för att förstå hur korrosion utvecklas i verkliga konstruktioner. Användningen av pålagd spänning resulterar i skillnader i typ och distribution av korrosionsprodukter jämfört med naturlig korrosion. Studier av naturligt korroderade provkroppar är en nödvändig del för att överbrygga skillnaderna mellan den kunskap som erhållits från artificiellt korroderade provkroppar och tillämpning av denna på verkliga konstruktioner. I detta arbete studerades den strukturella effekten av kloridinducerad, naturlig korrosion hos betongkonstruktioner. Specifikt undersöktes tre forskningsfrågor. Först studerades vidhäftningshållfastheten hos naturligt korroderade släta armeringsstänger med hjälp av 3-punkts böjnings- och utdragsprov. Provkroppar togs från en bro som byggdes på 1930-talet. Vidhäftningshållfastheten som uppmättes i dessa prover var signifikant högre än den som erhölls i försök på liknande armeringsstänger i provkroppar producerade i laboratorier. Effekten av korroderande armeringsstål på vidhäftningshållfasthet påverkades av gjutposition och närvaro av armeringsbyglar. Finita elementanalyser användes för att ytterligare undersöka sambandet mellan vidhäftning och glidning. Resultaten tydliggjorde hur balkarnas bärning påverkades av förlusten av vidhäftningshållfasthet när armeringsstålet flöt. Den andra frågan undersökte korrosionsprodukternas fördelning och egenskaper vid gränsytan mellan stål och betong - detta är relevant för att bedöma korrosionsskador i befintliga konstruktioner. Neutronskanning och röntgen användes för att erhålla kvalitativa och kvantitativa data om korrosion i en naturligt korroderad provkropp, inklusive volymförhållandet mellan stål och rost. I jämförelse med en artificiellt korroderad provkropp påvisades skillnader i korrosionsprodukternas fördelning. Slutligen studerades korrelationen mellan tvärgående sprickors sprickbredd och korrosionsskador. Data sammanställdes från experiment tillgängliga i litteraturen. I de utvalda studierna ingick balkar, förspräckta i 3-punktsböjning, utsatta för klorider i laboratoriemiljö. Ingen korrelation mellan sprickvidd och korrosion kunde påvisas, men gropfrätningar fanns med större sannolikhet i närheten av tvärgående sprickor. Sammanfattningsvis belyser detta arbete korrosionsprocessens komplexitet. En grundläggande förståelse av de material- och miljöegenskaper som påverkar denna process är nödvändig för att korrekt kunna bedöma befintliga konstruktioner. Försök på naturligt korroderade konstruktioner är ett grundläggande steg mot att förvärva denna kunskap.

Riassunto

La corrosione delle barre di armatura nelle strutture in cemento armato é, senza alcun dubbio, il meccanismo di deterioramento piú comune, nonché quello che comporta un maggior rischio per la vita utile della struttura. Ció non ostante la valutazione delle strutture esistenti é impegnativa a causa della natura complessa del processo di corrosione. Ció é in parte dovuto alla necessitá di adattare risultati ottenuti da esperimenti condotti in laboratorio, di breve durata alla complessa realtá delle strutture esistenti. Per condurre test di breve durata, é possibile imporre il passaggio di corrente tra la barra di armatura, che svolgerá nella sua interitá la funzione di anodo, e un secondo metallo esterno, in funzione di catodo. Questa riduzione dei tempi, che nel caso della corrosione naturale sono nell´ordine di decennni, ha dei lati negativi, poiché risulta in una distribuzione e composizione diversa della ruggine. Inoltre, certe caratteristiche del calcestruzzo, come la presenza di fessure transversali o il rapporto acqua/cemento, influenzano diversamente il processo corrosivo in condizioni artificiali rispetto alle condizioni naturali. Lo studio di campioni in calcestruzzo corrosioni naturalmente offre la possibilitá di connettere i risultati ottenuti da esperimenti a breve termine condotti in laboratorio con l´applicazione alle strutture esistenti. Questi campioni possono essere estratti da strutture esistenti, come nel caso di questa tesi, dove campioni sono stati estratti da un ponte costruito negli anni 30 per analizzare l´effetto dei danni da corrosione sulla capacitá di ancoraggio delle barre lisce. Gli esperimenti condotti hanno mostrato una capacitá di ancoraggio ampliamente maggiore rispetto a studi precedenti, dove le barre erano state corrose artificialmente. Línfluenza dei danni da corrosione sulla capacitá di ancoraggio presentava invece caratteristiche simili a quanto precedentemente osservato. Un altro campione, estratto dalla stessa struttura, é stato usato per analizzare la distribuzione dei prodotti da corrosione naturale utilizzando metodi non-distruttivi (neutron imaging e X-Ray CT). I risultati sono stati comparati con un campione artificialmente corrososo, e sono state osservate differenze in distribuzione e solubilitá dei prodotti della corrosione. Infine, l'effetto delle fessure trasversali sul processo di corrosione nelle strutture esposte in ambienti aggressivi contenenti cloruri é stato studiato attraverso la composizione di un dataset, ottenuto da dati disponibili in letteratura, e lápplicazione di metodi statistici sul medesimo. Non é stata trovata alcuna correlazione tra apertura di fessura e caratteristiche della corrosione delle barre di armatura. Per concludere, questo lavoro mette in evidenza la complessità del processo di corrosione e sostiene che per valutare adeguatamente le strutture esistenti è necessaria una comprensione approfondita del materiale e delle caratteristiche ambientali che influenzano questo processo. I test su strutture naturalmente corrose sono un passo fondamentale verso l'acquisizione di questa conoscenza.

List of Publications

This thesis is based on the following publications:

Paper A

[A] Karin Lundgren, **Samanta Robuschi**, Kamyab Zandi, "Methodology for testing rebar–concrete bond in specimens from decommissioned structures". *International Journal of Concrete Structures and Materials*,vol. 13, no. 38, 2019.

Summary of the paper This paper describes a methodology to select and design tests of the bond and anchorage between reinforcement bars and concrete in deteriorated specimens taken from decommissioned structures. The presented methodology is exemplified in the design of three test series on edge beams from two bridges; two series resulted in beam test set-ups and one in direct pull-out tests.

Contribution of the author The author participated in the planning of the paper and also in the planning and execution of two of the three presented examples of experimental series. The author contributed to the writing of the sections regarding those experiments, and with comments and discussions on the remaining paper.

Paper B

[B] **Samanta Robuschi**, Karin Lundgren, Ignasi Fernandez, Mathias Flansbjer, "Anchorage of naturally corroded plain reinforcement bars in flexural members". *Materials and Structures*, vol. 53, no. 38, 2020.

Summary of the paper In this paper, 20 beams with naturally corroded plain bars and varying amount of damage were taken from an 80-year-old bridge and tested in three-point bending to study the influence of corrosion on the anchorage capacity of plain bars. Loss of bond at yielding was observed to influence the load-carrying mechanism, which changed from beam to arch action. The casting position of the bars was identified as an important factor influencing bond strength.

Contribution of the author The author composed the literature study, participated in the planning, and was responsible for the execution of the experimental program. The author performed the analysis of the data, participated in the discussion of the results, and took responsibility for the planning and writing of the paper.

Paper C

[C] **Samanta Robuschi**, Jakob Sumearll, Ignasi Fernandez, Karin Lundgren, "Bond of naturally corroded, plain reinforcing bars in concrete". *Structure and Infrastructure Engineering* vol. 17, no. 6, pp. 792-808, 2020..

Summary of the paper In this paper, 156 pull-out tests were performed on naturally corroded, reinforced concrete specimens with plain bars sourced from a decommissioned bridge. The effect of corrosion on the bond strength and the amount of visible damage were found to be influenced by the casting position of the reinforcing bars. The presence of stirrups influenced the post-peak behaviour and helped maintain bond strength in the presence of cracks and spalling damage.

Contribution of the author The author composed the literature study, and participated in the planning of the experimental work. The author took the lead in the analysis of the data, participated in the discussion of the results, and took responsibility for the planning and writing of the paper.

Paper D

[D] Xiaotong Yu, **Samanta Robuschi**, Ignasi Fernandez, Karin Lundgren, "Numerical assessment of bond-slip relationships for naturally corroded plain reinforcement bars in concrete beams". *Engineering Structures* vol. 239, 2021..

Summary of the paper In this study, non-linear finite element analyses (NLFEA) were carried out to study the bond behaviour of nine naturally corroded specimens with plain bars, tested in 3-point-bending in previous work. Two different, one-dimensional (1D), bond-slip relationships were calibrated for each tensile bar in the tests, to account for loss of bond upon yielding. The loss of bond at yielding and yield penetration asymmetry were observed to be important factors for adequately describing structural behaviour.

Contribution of the author The author provided the experimental data and contributed with guidance to the finite element analyses. The author took part in the planning of the manuscript, provided the comparison with further experimental results (pull-out tests), and contributed to the writing of the paper.

Paper E

[E] **Samanta Robuschi**, Alessandro Tengattini, Jelke Dijkstra, Ignasi Fernandez, Karin Lundgren, "A closer look at corrosion of steel reinforcement bars in concrete using 3D neutron and X-ray computed tomography". *Cement and Concrete Research*, vol. 144, n. 106439, 2021..

Summary of the paper Multimodal neutron and X-ray tomography was used to observe the characteristics of corrosion products in two concrete samples. One sample was naturally corroded, extracted from an 81-year-old bridge, the other was corroded via the galvanostatic method, resulting in corrosion-induced cracks. Quantitative and qualitative data was acquired, including the iron-to-rust volumetric ratio in macroscopic interfacial voids and the thickness of the corrosion layer at the steel concrete interface.

Contribution of the author The author composed the literature study and contributed to the planning of the experimental program. The author participated in all the experimental work, and was responsible for the part of the experimental work conducted at Chalmers. The author performed the analysis of the data, participated in the discussion of the results, and took responsibility for the planning and writing of the paper.

Paper F

[F] **Samanta Robuschi**, Oscar Larsson Ivanov, Mette Geiker, Ignasi Fernandez, Karin Lundgren, "A statistical study of the impact of cracks on chloride-induced reinforcement corrosion". *To be submitted.*

Summary of the paper The influence of transversal cracks on chloride-induced corrosion characteristics and distribution was investigated. Hypotheses were formulated based on existing literature, and tested using statistical methods on a dataset compiled from experimental data available in literature. No clear correlation between surface crack width and corrosion characteristics was found, but corrosion pits were shown to likely appear in the proximity of transveral cracks. Concrete cover and water/binder ratio were observed to have an influence on corrosion rate and distribution.

Contribution of the author The author composed the literature study and made the first draft for the formulation of the hypotheses. The author collected and organized the data for the dataset. The author performed the analysis of the data, participated in the discussions of the results, and took responsibility for the planning and writing of the paper.

Other publications by the author

Other publications by the author, not included in this thesis, are:

[G] **S. Robuschi**, "Anchorage of naturally corroded, plain bars in Reinforced Concrete structures". *Licentiate Thesis. Chalmers University of Technology*, Göteborg, Sweden, April 2019.

[H] **S. Robuschi**, K. Lundgren, I. Fernandez, "Vad kan man lära sig av en 80-årig bro från Gullspång?". Bygg & Teknik, vol. 7, n. 19, pp. 42-45, 2019.

[I] **S. Robuschi**, I. Fernandez, K. Zandi, K. Lundgren, "Assessment of the load-carrying capacity of existing structures with corroded smooth reinforcement bars". *XXIII Nordic Concrete Research Symposium*, Aalborg, 2017.

[J] **S. Robuschi**, K. Lundgren, I. Fernandez, K. Zandi, M. Flansbjer, "Anchorage capacity of corroded smooth reinforcement bars in existing reinforced structures". 12^{th} *fib International PhD Symposium in Civil Engineering*, Prague, 2018.

[K] **S. Robuschi**, I. Fernandez, K. Lundgren, "Corrosion of naturally corroded, plain reinforcing bars". *fib CACRCS DAYS 2020, Capacity Assessment of Corroded Reinforced Concrete Structures*, Parma, 2020.

[L] **S. Robuschi**, A. Tengattini, "Corrosion of steel in concrete seen through neutron and X-Ray tomography". Neutron News, 2021.

Acknowledgments

The work in this thesis was carried out from March 2017 to December 2021, at the Division of Structural Engineering, Department of Architecture and Civil Engineering at Chalmers University of Technology. The research was financially supported by Formas under grant 2018-05973, and BBT under grant TRV 2017/39084 and TRV 2019/108016. Some of the numerical simulations presented herein were performed on resources at the Chalmers Centre for Computational Science and Engineering (C3SE) provided by the Swedish National Infrastructure for Computing (SNIC). Neutron and X-ray tomography was carried out at the Institut Laue-Langevin at the D50T instrument, under grant UGA-57 and UGA-78.

I would surely not have been able to make it this far without the help of my supervisors, Professor Karin Lundgren, Associate Professor Ignasi Fernandez and Professor Mette Geiker. Their passion for this work is inspiring, and working with them has been a pleasure and an honour. Karin, thank you for your constant encouragement, for sharing and discussing ideas with me, and for the continuous feedback. Ignasi, thank you for the passion you bring to every project you are involved in, and for being always ready to discuss whatever stupid question I have. And Mette, I believe your contribution has been fundamental in the last years of this work, I am very grateful for your help and support.

I would also like to thank Oskar Larsson Ivanov, for patiently helping me understand statistical analysis, for his precious feedbacks and support. I would not have been able to navigate the complex word of image analysis without the help and support of Jelke Dijsktra and Alessandro Tengattini. It has been a pleasure to work with you. Finally, I am very greatful for the help I received during my second year from visiting students Xiaotong Yu and Jakob Sumearll: it has been genuinely fun to work with you. I would as well like to thank Mathias Flansjber and Kambyab Zandi, who helped me in the start of my PhD project. I would like to thank the members of the reference group, for the good ideas and valuable discussions. Finally, special thanks go to Research Engineers Sebastian Almfeldt and Andres Karlsson, for their invaluable help and infinite patience.

I am very grateful for having had amazing colleagues through all my stay at Chalmers. It has been an honour to meet all of the people that has come and gone through our division for the last five years. A special thanks goes to Carlos, Mattias, Natxo, and Adam, for sharing lunch and navigate through a pandemic with me, for the fruitful conversations and for never shying away from a cake. Finally, it has been a pleasure to meet the "new generation" of PhD students in the concrete structures group, Fabio and Andreas, this last year; I do hope you´ll enjoy these years at Chalmers like I did.

Last, but not least, I would like to thank my friends and family, those in Sweden

and those in Italy, for always being there for me. Cristina, Matteo, we may not see each other often, but you are always there when I need a friend. I believe I ended up choosing this path thanks to my dad: your interest in all that is technological and fun is and was always inspiring. Finally, to Felix: none of this would have had the same meaning without you. You make me a better person.

Gothenburg, December 2021

Samanta Robuschi

Contents

Part I

Overview

CHAPTER 1

Introduction

"It is a truth universally acknowledged that a reinforced concrete structure showing signs of corrosion damage is in want of assessment."
(Adapted from Pride and Prejudice [1])

1.1 Background

Corrosion damages are the most common cause of deterioration in reinforced concrete structures [2]. A clear indicator of the presence of corrosion damages in the reinforcement bars inside the concrete is the presence of corrosion-induced cracks and spalling of the concrete cover. However, that takes place towards the end of a long process, that starts with the penetration of aggressive substances in the concrete cover and ends with the need of repairing (or demolishing) the damaged structure. Not all corrosion damages are necessarily visible at the external surface of the concrete: large corrosion pits may form in the reinforcement bars without inducing cracking of the concrete [3], owing to the presence of macroscopic voids at the steel-concrete interface and/or highly soluble corrosion products. Additionally, the presence of corrosion-induced cracks itself does not easily allow to estimate the corresponding loss of cross-sectional area of the reinforcement bar [4]. These charac-

teristics often make it hard to assess corrosion damages based on visual observations only.

The corrosion process is commonly divided in two stages [5]: an initiation phase and a propagation phase. At the beginning of the service life of the structure, corrosion of the reinforcement bars is prevented by the alkalinity of the concrete medium, which favours the passivation of the reinforcement bars. Two substances are commonly responsible for the initiation of the corrosion process: carbon dioxide, unavoidably present in the atmosphere, and chlorides, which are generally a result of exposure to marine environment or de-icing salts. Carbon dioxide decreases the pH of the environment, allowing for the depassivation of the bar, while chlorides locally break down the passive layer. Corrosion products are then generated as a result of the reaction of iron molecules with oxygen and hydrogen.

Corrosion products, in general, occupy a larger volume than the steel they originate from. Cracking and spalling of the concrete cover results from the volume expansion of the corrosion products, which applies increasing radial pressure at the steel/concrete interface [6]. Corrosion-induced cracks decrease bond strength [7], and increase the availability of oxygen and hydrogen at the steel/concrete interface, thus possibly increasing the corrosion rate of the bar [8]. Additionally, the strength and ductility of the bar decreases with the loss of cross-sectional area caused by the corrosion process [9], [10]. Hence, corrosion impairs the structural behaviour, and therefore the safety of RC structures [11], [12].

Corrosion damages result often in a need for the demolition or reparation of a structure, when currently in use assessment methods cannot show its safety. Additionally, within the last few decades, a number of structural failures have been attributed to undetected or underestimated corrosion damages [13]. A comprehensive understanding of the corrosion process and its associated structural effects is therefore essential to assure the safety of a structure, as well as to reduce the economical and environmental impact of unnecessary demolitions and reparations.

This work focuses on structural damages resulting from natural corrosion in chloride environments. Specifically, it focuses on structures where the availability of oxygen in the surrounding environment is not a limiting factor for the corrosion rate, i.e. structures that are not submerged. Natural, chloride-induced corrosion in reinforced concrete structure is here defined as corrosion resulting from the exposure of the structure to solutions containing chlorides, without the use of impressed current. In existing structures, the presence of chlorides is typically due to exposure to de-icing salts or marine environment. However, laboratory tests where specimens are exposed to a water/salt (NaCl) solution are as well included in parts of this work.

A common critique to existing research on corrosion damages is, in fact, the extensive use of corrosion methods where the corrosion process is accelerated using

impressed current. The corrosion process of reinforced concrete structures can take decades before the formation of substantial damages in the structure, therefore the use of such methods is often seen as the only option to study the structural behaviour of corroded structures. Results from accelerated corrosion tests are, however, not always immediately comparable to studies on naturally corroded specimens [7], [14]–[16]. Accelerated methods cannot reproduce the same corrosion mechanisms that take place during natural corrosion, being the anode and cathode location predetermined. It is therefore important to complement and compare these studies with observations and tests on naturally corroded structures, to understand their limitations and usability.

1.2 Aim of research

The aim of this research was to investigate the structural effects of natural, chloride-induced corrosion in reinforced concrete structures. Within this area, three main questions were formulated and addressed:

1. How does natural corrosion influence the bond and anchorage of plain reinforcement bars? Specifically:
   - What is the effect of corrosion damages on the bond capacity of naturally corroded, plain reinforcement bars?
   - How can laboratory tests be designed to study the anchorage capacity and bond of corroded plain bars, using parts of decommissioned structures as specimens?
   - Which factors are significant to define the bond-slip behaviour of corroded plain bars?
2. Which characteristics of the corrosion products and the surrounding concrete are relevant to assess and predict corrosion damages in existing structures? Specifically:
   - Which characteristics are of importance for modelling the corrosion cracking process?
   - How can these characteristics be estimated using non-destructive methods?
   - How do corrosion products and their distribution differ between artificially and naturally corroded samples?
3. Crack widths are strictly regulated in codes. Is this a proper way to ensure the desired structural behaviour over the lifetime? Specifically:
   - When, and how, do load-induced cracks influence the corrosion development, both in the initiation and propagation phases?

- How is surface crack width correlated to corrosion damages, and to the extent of such damages? Are there cases where surface crack width is not of importance?

1.3 Method

A schematic illustration of the methodology used in this work is presented in Figure 1.1. The work comprised three main experimental programs, designed based on the research questions defined in Section 1.2. Four different phases were identified in the work:

- In phase I, relevant literature was studied pertaining to the effects of natural corrosion on reinforced concrete structures. Knowledge gaps were identified, based on which the research questions outlined in Section 1.2 were formulated. The study was divided in three main parts, the first (**Q1**), investigating the effect of natural corrosion on the bond strength of plain bars, the second (**Q2**), characterising the corrosion products and the surrounding concrete, and the third (**Q3**), looking at the impact of load-induced cracks on corrosion patterns. After an extensive analysis of available literature, appropriate methods were selected.
- In phase II, the experimental campaign was designed. For each experimental program, adequate specimens from decommissioned structures were selected. The experimental campaign consisted of three main test programs: flexural tests and pull-out tests, as a mean to investigate the first research question, X-ray and neutron imaging studies, investigating the second research question. No experimental program is included for the study of **Q3**. The programs aimed at complementing each other with important data and information, to obtain a better overview of the structural effects of natural corrosion and contribute to filling up the gaps identified in literature.
- In phase III, the collected data were evaluated and interpreted. Different techniques were used for the different experimental programs, including Digital Image Correlation, Non-Linear Finite Element models, 3D scanning and image analysis. **Q3** was investigated using statistical methods.
- In phase IV, data from literature were collected, and compared to experimental findings.

Phase I was the very first phase of the work, and defined its structure. Then, for each experimental campaign, phase II followed. Phase III and IV were often conducted in parallel. The order of the research questions (Q1 to Q3) follows the chronological order of the studies.

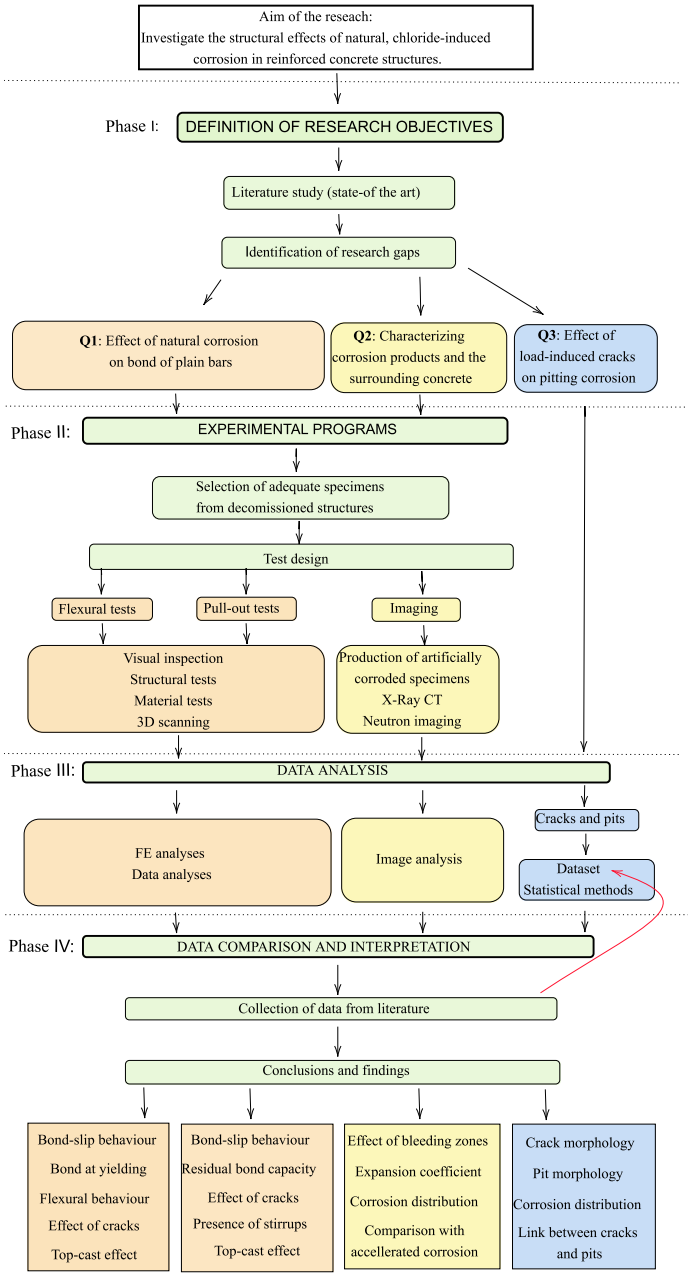

Figure 1.1: Overview of the methodology. Full formulations of research questions Q1-3 can be found in Section 1.2.

1.4 Scope and limitations

The scope and main limitations of the present work are summarized in the following. Scope and limitations apply both to the thesis and the appended papers.

- This work focuses on natural, chloride-induced corrosion in reinforced concrete structures. The studied structures are not in water saturated conditions (submerged structures), and carbonation, another common cause of corrosion damages, was not investigated.

- The bond and characteristics of naturally corroded plain bars were studied by taking specimens from the edge beams of a decommissioned bridge (**Paper B, Paper C**). The bridge was exposed to de-icing salts and freezing-thawing cycles. The obtained results are therefore likely representative of similar exposure environment, and also concrete and steel properties, but cannot be generalized without further research.

- Structural tests on specimens from decommissioned structures imply the need to adapt the test set-up to the specific geometry of the structure, which sometimes results in non-optimal solutions. This may affect the interpretation of the results. Although all the specimens in this work were carefully handled, possible disturbances to the steel-concrete surface may have been induced by cutting and/or drilling to shape the test specimens from the original decommissioned edge beams (**Paper B, Paper C, Paper E**), by the presence of support pressure acting on the anchorage of the plain bars during the flexural tests (**Paper B**), and by drilling into the reinforcement bars in the pull-out test set-up (**Paper C**).

- The imaging study was carried out on two samples, one naturally corroded and the other corroded via the galvanostatic method (**Paper E**). The main aim of the study was to investigate the applicability of the selected non-destructive methods to detect and quantify corrosion characteristics. However, the quantitative results obtained from the studied samples cannot be generalised: the natural corroded sample was representative only for its specific exposure condition and material properties, and the type and distribution of the corrosion products in the artificially corroded sample was influenced by the current density applied and the material properties of the sample.

- The effect of transversal cracks on the corrosion process was studied based on existing literature, and limited to load-induced cracks induced in 3-point-bending tests. Other types of cracks, e.g. restrained shrinkage, have different shapes and therefore their influence on the corrosion process may change.

1.5 Original features

The original features of the present work are summarized as follows:

- This work looks into natural corrosion through decommissioned structures, with special focus on the bond of naturally corroded plain bars. To the author's knowledge, this has not been done before.
- A test set-up for carrying out pull-out tests from parts of existing structures was designed, and the obtained bond-slip data were compared to results from flexural tests on specimens taken from the same structure.
- Neutron imaging was used, for the first time to the author's knowledge, to quantify corrosion characteristics in reinforced concrete structures.
- Data on chloride-induced corrosion from previous research was collected and organized in a dataset. Statistical methods were used to identify important factors influencing the size and distribution of corrosion pits.

1.6 Outline of the thesis

This thesis consists of an introductory part and six appended papers. The former is divided into six chapters:

- In chapter one, the background to the work is given, and aim, methods, scope and limitations, and original features are presented.
- In chapter two, the knowledge necessary to establish the theoretical framework on which this work is based is given. Specifically,the corrosion process and its structural effects are presented, together with an overview of relevant works from literature.
- In chapter three, an overview of the work that followed research question 1 (**Q1**) is given.
- In chapter four, an overview of the work that followed research question 2 (**Q2**) is given.
- In chapter five, an overview of the work that followed research question 3 (**Q3**) is given.
- In chapter six, the main conclusions drawn from this work and suggestions for future research are given.

Finally, Fig.1.2 gives a visual overview of the content of the appended papers presented in this thesis (see Fig. 1.1).

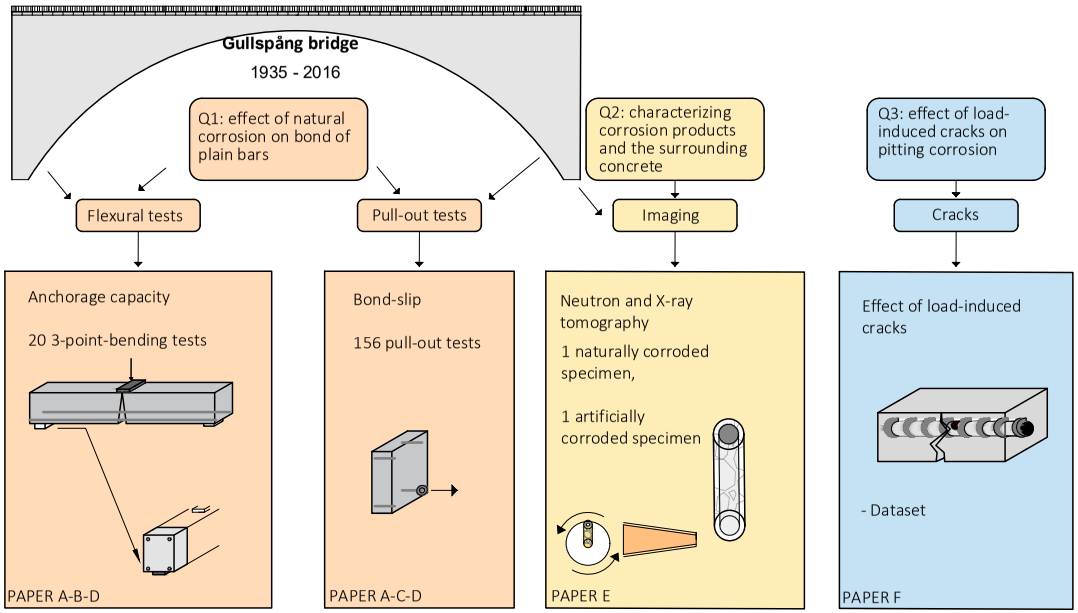

Figure 1.2: Overview of the work presented in this thesis and the related publications. Full formulations of research questions Q1-3 can be found in Section 1.2.

CHAPTER 2

Theoretical background

All uncorroded reinforcement bars are alike;
each corroded reinforcement bar is corroded in its own way.
(Adapted from Anna Karenina[17])

This chapters aims at giving theoretical background to the present work. Three main questions have already been presented in Section 1.2: these questions follow the chronological order of the study; this chapter follows instead the chronological steps of the corrosion process, from initiation to propagation. It opens with an overview of the corrosion process, its causes, phases and influencing factors: these topics are the object of the second (Q2) and the third (Q3) research questions. An overview of structural damages follows, and specifically, the effects of corrosion on the bond of plain reinforcement bars, which is the object of the first research question, and the effects of pitting corrosion. Pitting corrosion, how it forms and how it is influenced by material and environmental characteristics, is the object of questions two and three.

2.1 Corrosion of steel in concrete

The first use of iron-reinforced concrete dates back to 1853. In 1904, the first skyscraper using reinforced concrete was built in Cincinnati. The introduction of iron (and later steel) reinforcement in concrete was revolutionary: reinforcement bars compensated for the low tensile strength of plain concrete, and, at the same time, the alkaline environment of concrete resulted in the passivation of steel, thus preventing the bars from corroding. Initially, reinforced concrete was seen as the perfect mean to make steel last forever [18].

It was much later, approximately in the decade between 1960 and 1970, that doubts over the durability of reinforced concrete started to emerge [18]. In the following years, corrosion of the reinforcement bars became increasingly of interest among researchers, and in the 1980s the concept of service life was introduced [5]. Consequently, new regulations were added to building codes, limiting crack openings [19] and prescribing minimum concrete covers (e.g. ACI 357R-84 [20]). The third research question formulated in this work (Q3) explores the relation between these regulations and corrosion prevention. Nowadays, reinforced concrete (RC) structures are well known to be vulnerable to deterioration, among which corrosion of the reinforcement bars resulting from chloride-contamination is known to be the most common [21].

Corrosion mechanisms

Corrosion of steel in concrete is an electrochemical process [22]. Reinforcement bars in concrete are protected from corrosion by the alkaline pore solution of the concrete, and by the concrete surrounding the bar itself, that provides a physical barrier against aggressive substances [23].

The pore solution of concrete has, normally, pH values between 12 and 14. High alkalinity, if oxygen is available, results in the formation of an iron-oxide layer on the surface of the steel, known as passive layer, that reduces the exchange of ions between the steel and the surrounding concrete. The corrosion process is thus slowed down to a negligible rate [24]. Hence, if the concrete is uncontaminated, concrete structures, have, in general, good durability against corrosion of steel reinforcements.

Nevertheless, corrosion of steel reinforcements is the major deterioration process in reinforced concrete structures. Corrosion initiates when the passive layer is damaged, usually following either a reduction of the pH of the pore solution or chloride-attack [13]. In those areas where the passive layer breaks down, the speed of the corrosion process increases. Two main causes are recognised: carbonation and chloride contamination, which are further explained in the next section. Other less common causes are sulphide ion attacks or stray DC currents [25].

The time frame in which carbonation or/and chloride contamination take place is generally known as the initiation phase of the corrosion process, according to Tuutti's model [5]. Tuutti's model describes the service life of concrete with respect to degradation due to corrosion and has been commonly used since first published in 1982. The model divides the corrosion process in two phases: initiation and propagation, see Fig. 2.1.

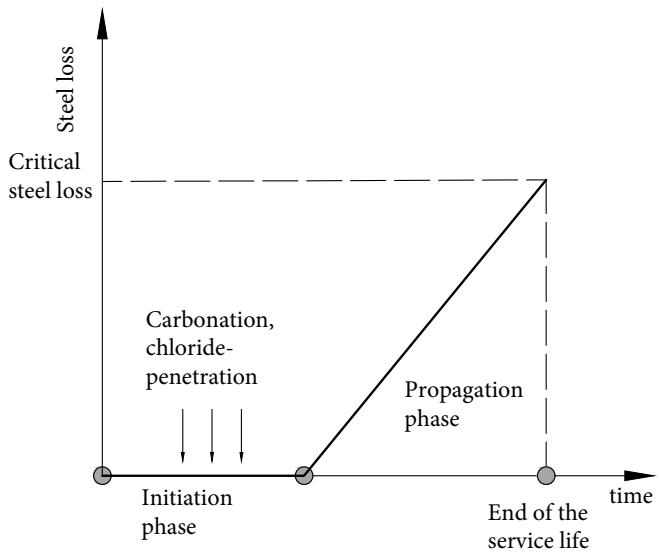

Figure 2.1: Tuutti's model for reinforcement corrosion, adapted from [5]

Corrosion initiation

The corrosion initiation phase corresponds to the ingress of aggressive substances and can be defined as *the transition from a stable passive state to a state where active corrosion is not only possible, but also occurs at a certain minimum rate to lead to at least some signs of corrosion* [26].

Hence, the corrosion initiation phase deals with two well-defined questions:

- What starts the corrosion process?
- How long does it take for the corrosion process to start?

As for the first question, we have already pointed to chloride contamination and carbonation.

Carbonation is the result of the reaction between CO_2 from the air and calcium-containing phases in concrete. The main reaction consumes, among others, calcium hydroxide and produces calcium carbonate, decreasing the pH of concrete. Carbonation starts at the external surface of the structure, and eventually the carbonation front may reach the reinforcement bars. Generally, the carbonation front reaches relatively large areas of the reinforcement bars, resulting in a general type of corrosion. Carbonation is common in urban environments, and the extent of carbonation damages may worsen due to climate change [27], [28].

Recent studies have highlighted that assuming that corrosion starts when the carbonation front reaches the reinforcement bars due to the decrease in pH of the pore solution is too simplistic. Among the triggering factors, the moisture state is likely the most important [26]. Therefore, it may be possible to allow e.g. dry concrete structures to carbonate. This would promote the use of more environmentally friendly cementitious binders, improve fiber reinforced composites [29], and could even have a good environmental impact, since carbonation removes carbon dioxide from the atmosphere.

Chloride-induced corrosion is a common deterioration mechanism in structures exposed to sea-water or de-icings salts. The corrosion resulting from this process is generally characterized by local pits and large uncorroded areas: the local corrosion rates can thus be considerably higher than for corrosion initiated by carbonation. Chlorides can penetrate the concrete cover through different transport mechanisms, which can be roughly divided into transport through the porous media and transport through cracks. Transport in the bulk material can take place through four main mechanisms: capillary suction; permeation driven by a pressure gradient; diffusion driven by a concentration gradient; and migration due to the presence of an electrical field [13].

The main barrier against pitting corrosion is given by the passive film and the depth of the concrete cover [3]. The passive film remains stable until chloride ions reach the steel surface. The pitting potential (the least positive potential at which pits can form), has been observed to decrease with increasing chloride/hydroxide (Cl^-/OH^-) ratios, though other parameters, as e.g. pre-passivation time, affect this value [3]. Additional factors influence the process, e.g presence of cracks, concrete characteristics (water/binder ratio and cement type), and presence of interfacial air voids, local defects, and bleeding zones have been strongly associated with susceptibility to corrosion initiation [3].

Corrosion of the steel reinforcement bars does not initiate before a certain amount of chlorides is present at the steel-concrete interface [30]. This amount of chlorides is generally referred to as *critical chloride content*, and has been the object of numerous studies in recent years, e.g. [31]–[34]. The time to corrosion initiation is traditionally estimated by predicting the evolution of the chloride content at the steel-concrete

interface and comparing it against a known threshold (see Fig. 2.2). However, both these predictions involve large uncertainties, and particularly no agreement on threshold values is found in literature [16], [35].

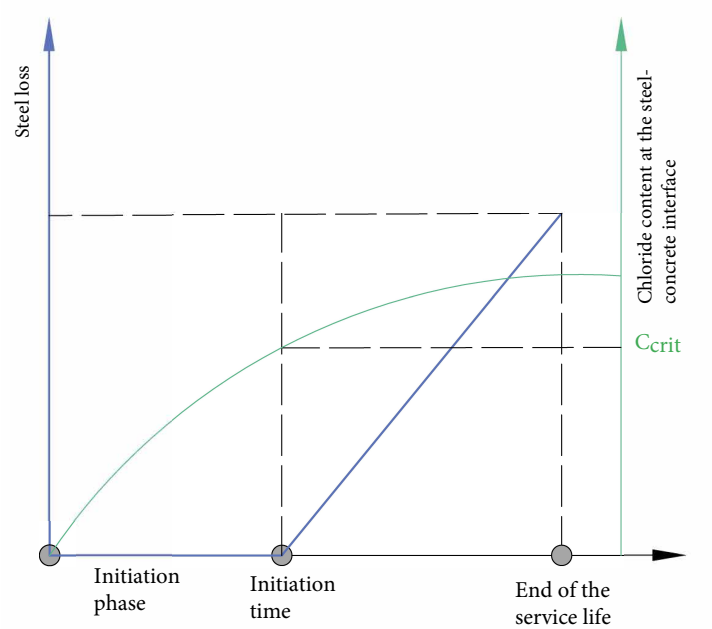

Figure 2.2: Generally assumed relationship between the chloride content at the steel-concrete interface and the corrosion initiation phase, adapted from [16]

The actual initiation point of the corrosion process is nowadays acknowledged not to be an instantaneous event [36]. In Fig. 2.3, Tuutti's diagram is re-proposed, as adapted by Angst [16]. The initiation phase is now followed by a corrosion onset phase: during the onset phase, the corrosion rate of chloride-induced corrosion is highly dependent from the supply of chloride ions at the anode, and the steel may re-passivate when the supply of chlorides is not sufficient [37].

Corrosion propagation

The actual corrosion process starts in the propagation phase, and factors that determine the rate of corrosion define the length of this phase [5]. Once aggressive substances have reached the steel-concrete interface and damaged the passive layer,

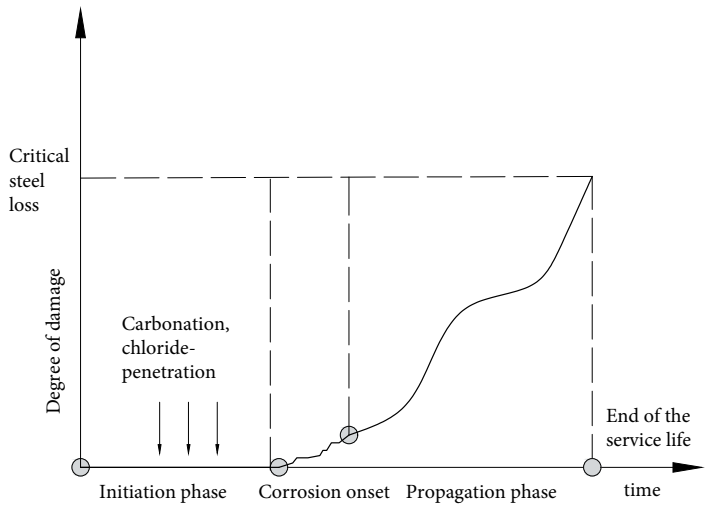

Figure 2.3: Adaptation of Tuutti's diagram, including corrosion onset and changes in the corrosion rate through the service life of the structure [16]

the rate of dissolution/corrosion of the steel might increase and corrosion products are generated as a result of the reaction of iron molecules with oxygen and hydrogen. Corrosion products occupy a volume larger than the steel they originate from. In case of sufficient oxygen, an increasing presence of corrosion products results in increasing radial pressure applied at the steel/concrete interface, and eventually leads to cracking and spalling of the concrete cover [6]. However, the presence of chlorides is expected to increase the solubility of corrosion products, to the point that chloride containing corrosion products in wet concrete may migrate through the paste instead of depositing at the steel-concrete interface. This significantly increases the time at which corrosion damages would manifest at the concrete surface, and constitutes a particularly risky scenario for flexural elements [38].

A number of factors influence the rate of the corrosion process: in uncracked concrete, the opening of corrosion-induced cracks, and later the spalling of the concrete cover, would accelerate the corrosion process. In cracked concrete, self-healing of cracks may reduce the corrosion rate, by reducing the flow of aggressive substances. Seasonal changes and changes of the exposure environment can as well change the corrosion rate [13], [39]. In Fig. 2.3, emphasis is given to the non-linearity of the propagation phase.

The length of the corrosion propagation phase, given its complex nature, and the high number of parameters and chemical reactions involved, is knowingly hard to predict [16]. Four partial processes are involved in the corrosion process of chloride-contaminated corrosion, and the rate of the corrosion process is commonly assumed to be limited by the slowest of the processes. However, different studies have observed different partial processes being the limiting factor [40].

Corrosion-induced cracking plays a major role when it comes to visual assessment of corrosion damages. Precipitation of corrosion products at the steel/concrete interface is expected to give rise to expansive stresses and lead to concrete cracking and spalling. The volumetric expansion of the corrosion products is described by the iron-to-rust ratio, and it is particularly important for defining the time from the initiation of the corrosion process to the formation of corrosion-induced concrete cracking. The iron-to-rust ratio of corrosion products without chlorides is expected to vary between 2.2 and 6.4 depending on the availability of oxygen and hydrogen at the time of formation of the corrosion products [41]. However, chloride containing corrosion products are expected to have increased solubility and lower volume [38].

The differences in expansion factors and solubility of the corrosion products are only the first obstacle for, on one hand, predicting the length of the propagation phase, and on the other, evaluating the loss of steel corresponding to the formation of corrosion-induced cracks. The increased solubility of corrosion products due to the presence of chlorides delays cracking by allowing corrosion products to diffuse through the pore system of the concrete instead of accumulating at the steel-concrete interface [42]. The presence of cracks can as well favour migration of corrosion products away from the steel/concrete interface [43]. Finally, the compressibility of rust itself is a significant factor in delaying time to cover cracking [44].

A number of models is available in literature to predict the formation of corrosion-induced cracks, however, due to gaps in the current knowledge, most are either empirically calibrated on experiments with impressed currents, or utilize fix values for the parameters describing certain characteristics of the corrosion products, disregarding material and environmental conditions, and thus have limited predicting power.

Chloride-induced corrosion

The main corrosion process taking place in chloride-contaminated reinforced concrete is generally known as 'macro-cell' corrosion. At the anodes, local pits form, which are very small in size compared to the uncorroded steel area (cathode). Two half-cell reactions take place, spatially separated from each other, hence the term 'macro-cell'. The distance is in the order of decimetres, or in some cases, even metres [40].

During the two half-cell reactions, electrons are produced at the anode through oxidation and consumed at the cathode. At the anode, the iron (Fe) is oxidized and dissolved into the surrounding solution ($Fe \longrightarrow Fe^{2+} + 2e^{-}$). At the cathode, oxygen is reduced ($H_2O + \frac{1}{2}O_2 + 2e^{-} \longrightarrow 2OH^{-}$) (Fig. 2.4).

Four partial processes are involved in the corrosion process (Fig. 2.4):

- The oxidation of iron at the anode (anodic process) that liberates electrons in the metallic phase and gives rise to the formation of iron ions whose hydrolysis produces acidity [13];
- the reduction of oxygen at the cathode (cathodic process) consumes the electrons and produces alkalinity.
- the transportation of electrons from the anodic to the cathodic region;
- the current flow in the bulk of the concrete, from the anodic to the cathodic regions, transported by ions in the pore solution (ohmic process).

Balance between these processes is assured by these reactions having the same rate. Hence, the slowest of the four partial processes determines the corrosion rate.

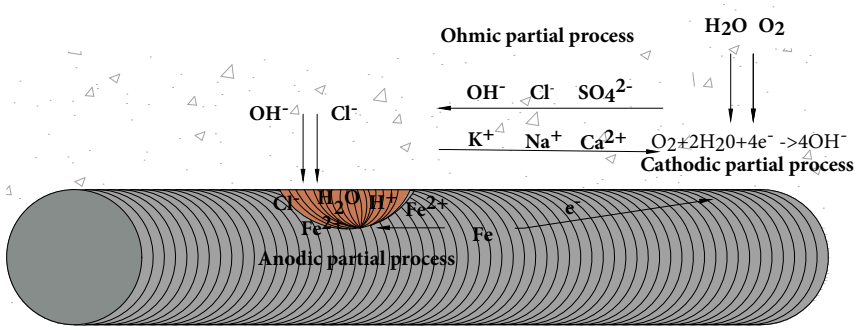

Figure 2.4: Partial processes involved in the corrosion process.

Artificial and natural corrosion

Artificial corrosion techniques are often used to simulate real-life corroded conditions in laboratory studies, and many corrosion models are based on findings obtained with these techniques. These techniques, such as impressed currents, are popular due to the substantially shorter exposure time needed for the specimens to corrode. It is

possible to generate an amount of corrosion products that would take 30-years to form naturally, in a matter of a few months in the laboratory. The most commonly used method for artificially inducing corrosion is the impressed current technique (or galvanostatic method). This technique applies a constant current from a DC source to the rebar embedded in concrete to induce corrosion. Chlorides are often used as depassivating substance, either by adding salt to the concrete during the mixing process or by exposing pre-cracked specimens to a highly concentrated salt solution.

Although the use of artificial corrosion has evident benefits, several uncertainties have been raised on how well it captures real-time corrosion formation, as it would occur naturally in RC structures. Various authors observed that different corrosion methods influenced the surface characteristics of the bar [45], the morphology [46], and the solubility [47] of the corrosion products. These changes influence the structural behaviour of the structure, and may therefore lead to an inaccurate understanding of the structural effects of natural corrosion. E.g. Saifullah and Clark [14] showed that differing current density has an effect on the bond strength.

Additionally, corrosion as a result of the galvanostatic method tends to present a more general corrosion pattern, whereas naturally corroded specimens commonly display more distributed pitting if chlorides are present. Austin *et al.* [48] observed differences in the electrochemistry behind natural and artificial, chloride-induced corrosion. The primary electrochemical difference from naturally corroded systems was the gradual reduction of the local pH due to electrolysis of the pore water. This may lower the critical chloride concentration required to induce corrosion and accelerate the degradation process [48].

Testing naturally corroded specimens taken from decommissioned structures offers an alternative to the use of artificial corrosion methods. Further, it allows for the study of corrosion damages as the results of the combination of many factors influencing the aging processes of RC structures, such as creep, and freezing-thawing cycles. Examples studies on naturally corroded specimens can be found in [7], [10], [49]. Testing naturally corroded specimens, however, comes with challenges, as, e.g. finding well-defined specimens, designing feasible test set-ups, and evaluating results with a large scatter due to the heterogeneity of the specimens.

2.2 Structural effects of corrosion in RC structures

The existence of many studies focusing on the corrosion process is motivated by the structural effects of corrosion of RC structures, that often imply a loss of safety and function for the structure [7], [11], [12].

Corrosion affects RC structures in two, main ways:

- Corrosion changes the reinforcement bar geometry by reducing the cross-sectional area of the bar. This leads to a reduction of its mechanical properties, strength and ductility [9], [10];
- Corrosion products, generally, occupy a larger volume than the uncorroded steel. This introduces pressure between the bar and the surrounding concrete. As the corrosion products continue to develop, this pressure may induce cracking and, later, spalling of the concrete cover [6];

Numerous studies on the various structural effects of corrosion exist, from the effects on the reinforcements bars, see e.g. [9], [10], [50], to the serviceability state, where corrosion affects deflections and stiffness (and thus, load redistribution), see e.g. [51], [52]), to the ultimate state, where the effects on the load-carrying capacity are studied in terms of bending capacity, shear capacity, and anchorage [11], [53], [54]. Bending and shear capacities are reduced due to the reduction of the rebar cross-section, a decrease in the effective depth due to spalling of the concrete cover, and changes in the bond conditions. Crack widths and deflections are affected by changing tension stiffening, linked to the degraded bond. The deformation capacity of the structure is impaired by highly localised damage resulting in a localisation of deformations. Finally, corrosion may lead to changes in the failure mechanism, from ductile, as designed, to brittle [55]. In Fig. 2.5, an overview of the structural effects of corrosion is given (adapted from [25]).

This study identifies three different gaps in the current knowledge about the structural consequences of corrosion. The first research question (Q1) looks into the effect of natural corrosion on the bond of plain bars: the difference in bond mechanisms between plain bars, an old type of reinforcement bars, and deformed bars, as in use nowadays, suggests that the effect of corrosion damages may as well differ. The second and third questions focus on pitting corrosion. Pitting corrosion, by locally reducing the cross section of the bar, may limit ductility and bending capacity. This is particularly dangerous if there are no visible signs of corrosion. The research questions look into influencing factors for the formation of pitting corrosion, such as the presence of a bleeding zone (Q2) and load-induced and restraint cracks (Q3). The questions look as well into non-destructive methods for the study of pitting corrosion, predictive models (Q2) and current code regulations to ensure durability of concrete structures (Q3).

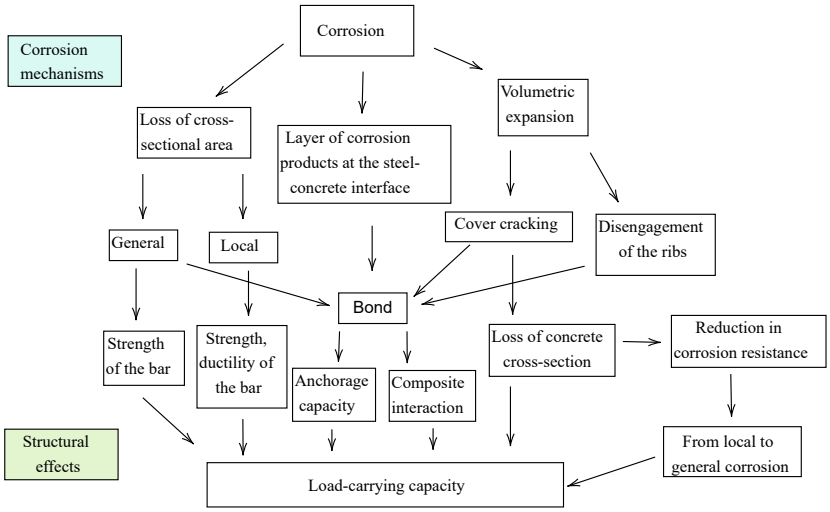

Figure 2.5: Corrosion process and its structural consequences, adapted from [25] and [56].

Effect of corrosion on the bond of ribbed bars

Composite action is achieved in RC members by the bond between reinforcement bars and concrete. In the interaction zone, stresses are transferred between the concrete and the reinforcement bar. Their bond is the result of three different mechanisms: chemical adhesion, friction, and mechanical interlocking between the ribs of the reinforcement bars and concrete [6]. The latter provides the largest contribution to the bond strength; the bearing action of the ribs transfers inclined forces to the concrete. These forces are generally divided into a longitudinal component (bond), and a normal component (splitting stress). The splitting stress resulting from bond action can result in splitting failure, while pull-out failure originates from the failure of the concrete between the ribs. Bond characteristics are generally dependent on several parameters, including concrete strength, positioning, type and amount of reinforcement bars, as well as concrete cover [57].

Corrosion damages include the formation of corrosion induced cracks and the formation of a weak layer of corrosion products at the steel-concrete interface. These two effects influence the bond between the steel and the surrounding concrete. However, Cairns *et al.* [58] performed a study on the changes in friction characteristics of the interface between corroded reinforcement and concrete using artificial corrosion

methods; the results indicated that the presence of corrosion products does not impair friction characteristics for specimens showing less than 1.0 mm surface cracks. Thus, it was concluded that volumetrical expansion is the effect of corrosion having the highest impact on bond strength.

Volumetric expansion affects the bond between the bars and the surrounding concrete in different ways: if no cracks are present in the anchorage region, the increase in mechanical pressure provided by the corrosion products will noticeably increase friction, as friction is a function of the normal stresses on the steel/concrete interface [59]. There is a limit, however, to this phenomena, in that excessive pressure is likely to crack the concrete cover and consequently lead to a loss of confinement [60], [61]. Blomfors *et al.* [62] give an overview of the effects of corrosion on the bond-slip curve of deformed reinforced bars.

Effect of corrosion on the bond of plain bars

Plain bars are an old type of reinforcement bars, i.e. reinforcement bars with a smooth surface. The first RC structures were constructed with plain bars. Plain bars were replaced with the introduction of deformed bars, which improved the bond between the steel and the surrounding concrete thanks to the presence of ribs. The use of deformed bars in RC constructions became common during the mid-1900s, though implementation differed between countries: Sweden adopted them in the 1940s, Canada, USA, and Australia in the mid-1950s, and Italy maintained use of plain reinforcement bars for about 20% of RC structures through the 1980s [63].

The bond of plain reinforcement bars, having no contribution from the ribs, relies mostly on adhesion and friction for transferring forces; mechanical interlock takes place only on a micro level, between the concrete and the surface roughness of the steel bar. Friction, being a function of the normal stresses on the bar, increases with increasing confinement, and, as a result, the bond capacity of plain reinforcement bars depends on the level of confinement of the bar itself [6] (Fig.2.6). Sliding friction [64], as to indicate the wedging action of small particles of concrete detached by the initiation of the slip, contributes to the residual bond of plain bars.

Being the stress transferring between concrete and steel mostly carried out by friction, factors such as the density of the concrete surrounding the bar and, consequently, the casting position are expected to have high impact on the bond of plain reinforcement bars. Top-cast bars are more likely to be surrounded by less dense concrete. This is the result of settlement of aggregates below the bar and accumulation of bleed water at the bar [65]. Lower density results in lower bond strength than for bottom-cast bars [66], since decreased confinement reduces the normal stresses on the bar.

The presence of corrosion products has an initial beneficial effect on the bond

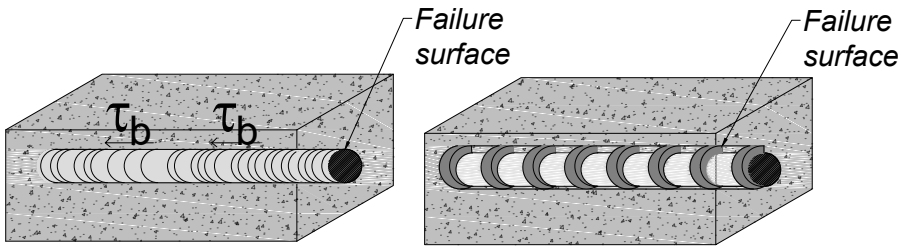

Figure 2.6: Failure surface: plain bars (left) and deformed bars (right) at pull-out.

of plain bars, by increasing normal stresses, and consequently, friction. In tests by Cairns *et al.* [66], the bond capacity of top-cast bars was shown to substantially increase with the introduction of small levels of corrosion. Artificially corroded bottom-cast bars, on the other hand, performed better in an uncorroded state, since they were more prone to crack, and thus, lose bond capacity with increasing corrosion level.

Research on the bond of corroded (and uncorroded) plain bars is limited. Formulas for the evaluation of the bond of uncorroded plain bars are available in Model Code 2010 [67], and in literature [68] [69] [70] [71] [72]. These equations are most commonly based on results of pull-out tests. In an attempt to appear consistent with deformed bars, many of these expressions are a function of the compressive strength of the concrete.

A possible problem with laboratory-made tests on the bond of plain reinforcement bars is the reproducing of the characteristics of a material no longer in use. Old reinforcement bars had, compared to those in use nowadays, low yield strength, high ductility and a remarked difference between yield and ultimate strength. Surface roughness is as well expected to be greater in old reinforcement bars [71]. Additionally, the difference in casting techniques for the concrete is likely to affect its density and homogeneity. Gustavson [73] studied the influence of concrete density and surface roughness on the bond behaviour of three-wire strands and found that an increase in the micro-roughness of the strand surface strongly increased adhesion in the initial bond response. The study on three-wire stands also determined a relationship between the bond strength of non-corroded bars with an increase of the concrete density. Support pressure (a supplemental source of compressive confinement of the reinforcing bars), has also been linked to increased bond strength [74].

Effect of bond deterioration on the behaviour of structural members

Bond deterioration has as a possible consequence anchorage failure of the structural member. This brittle failure mechanism was, e.g. studied for naturally corroded ribbed bars by Tahershamsi *et al.* [7], where a reduction in load-carrying capacity was observed to correspond to a reduction in bond strength in 4-point-bending tests failing in anchorage.

Cairns *et al.* [59] investigated the effect of corrosion on the behaviour of flexural members with plain bars. A consistent increase in strength was instead observed in the artificially corroded beams when compared to non-corroded specimens. The additional strength was attributed primarily to the initial increase in bond due to the volumetric expansion of the corrosion product inducing normal pressure. Most of the tested beams were subject to flexural failure, preceded by yielding of the tensile reinforcements. Towards the end of the test, the decrease in bond capacity due to yielding of the tensile reinforcement led to a change in the load-carrying mechanism, from purely flexural behaviour to a hybrid arching/flexural action. A similar behaviour was observed by Nasser *et al.* [75], who observed a reduction in the number of flexural cracks, and an increase in their widths linked to bond deterioration in specimens with plain bars tested in 3-point bending.

A similar mechanism was observed as well in studies by Dong *et al.* [76] and Feldman *et al.* [77]. Both studies investigated the influence of bond capacity on the failure mechanism of flexural beams. Dong *et al.* [76] performed 4-point bending tests on twenty, artificially corroded, RC beams with deformed bars. A transition from beam to arch action was observed in the later loading stages in connection to a degraded bond capacity in the bars due to corrosion. Feldman *et al.* [77] investigated the transition from beam action to arch action in flexural members with plain bars, observing bond strength distributions along the length of tensile reinforcements. High bond stresses were observed adjacent to the supports for beams where shear was carried principally by arch action. Arch action was associated with a marked reduction of flexural stiffness. The change from flexural to arch action can be explained by analysing the relationship between the shear force, V, and the bending moment, M, in a section x along the beam [76]:

$$V = \frac{dM(x)}{dx} \tag{2.1}$$

Considering $M(x)$ is equal to the force, $F(x)$, in the bar, multiplied by the lever arm, $z(x)$, equation 2.1 can be rewritten as:

$$V = \frac{dF(X)}{dx} z(x) + F(x) \frac{dz(x)}{dx} \tag{2.2}$$

The first term in equation 2.2 represents beam/flexural action: the force in the bar decreases outside the high moment region, while the lever arm is constant. Shear forces need to transfer from the reinforcement to the surrounding concrete through bond for beam action to occur. Low bond capacity limits the amount of beam/flexural action. The second term represents arch action: the decrease of the moment outside the high moment region is linked to the decrease of the lever arm, but the force in the bars is constant. Pure arch action does not involve the transfer of forces between the tensile reinforcement and the surrounding concrete. A decrease of bond capacity, due to, e.g., yielding of the tensile reinforcements or bond degradation, corresponds thus to a transition from beam action to arch action.

Pitting corrosion

Pitting corrosion in the reinforcing bars is common in structures exposed to aggressive chloride environments. Pitting corrosion is highly localised, and significant loss of cross-sectional area can take place at the anode, which is much smaller compared to the cathodic area. Pitting corrosion is non-homogeneous along a reinforcing bar, and its spatial variability is influenced by many factors, such as, to mention some, casting position [78], presence of early-age and load-induced cracks [79], local defects at the steel/concrete interface [80], [81], metallurgy and concrete characteristics [3].

Pitting corrosion results in a loss of ductility due to an uneven distribution of the cross-sectional area along the length of the reinforcing bar, and stress concentrations associated with the abrupt changes in geometry [82]–[84]. In a reinforcing bar with corrosion pits only the segment affected by pitting corrosion may yield before the bar fractures. In recent work, a critical corrosion level was defined, depending on the ratio between the ultimate and the yield strength: once a pit has reached the critical corrosion level, yielding localises at the pit, and the yield length does not extend to the rest of the bar [50]. This can significantly change the flexural behaviour of the structure [85].

2.3 Prevention and monitoring of corrosion damages

Corrosion of reinforcement bars affects the structural behaviour and overall safety of reinforced concrete structures. Consequently, it is important to have good design strategies (e.g. through regulations in building codes) to delay and prevent such damages. Additionally, it is important to have effective means to monitor the evolution of the corrosion process in existing structures.

Code regulations

Surface crack width is currently regulated in codes as a way to prevent corrosion. The reinforcement bar layout is typically chosen in a way that the expected cracks will be transverse to the placement of the reinforcing bars, thus the surface crack width of transverse cracks is often the object of studies linking surface crack widths to corrosion damages.

It is generally accepted in literature that the presence of transverse cracks reduces time to corrosion initiation [86]. This is because the cracks offer a preferential route for potentially hazardous substances, such as chlorides and carbon dioxide, to reach the reinforcing bar. Regulating surface crack width is expected to decrease the flow of these substances to the reinforcing bar, and thus increasing the service life of the structure.

Codes contain semi-empirical and empirical formulas to estimate surface crack widths at different loading stages. Maximum values for the allowable surface crack width are given for different exposure environments, [87]. This implies assuming a correlation between surface crack width and corrosion damages in the reinforcing bar, specifically that an increase in surface crack width increases the probability of corrosion in the reinforcing bars. However, numerous research efforts have not been able to confirm such correlation [88]. In 1979, A. W. Beeby wrote: "*It should also be noted that, from the point of view of corrosion control, the permissible crack width of 0.3 mm specified in CP110 (or indeed any other width) cannot be justified in any logical way from test evidence: it is simply a guess*" [89]. Though it is widely accepted that cracks in concrete offer a preferential way for chlorides to reach the reinforcement bars, the influence of surface crack width is thus still highly debated.

An interesting aspect of the choice of limiting surface crack width is that such limitation may be contradictory with respect to the corrosion-delaying effect of the concrete cover [90]. If we look at the case of bending cracks, surface crack width increases with the concrete cover for the same crack opening at the steel-concrete interface: to decrease surface crack width, a small concrete cover may therefore be beneficial. However, increasing the depth of the concrete cover is expecting to delay corrosion initiation and propagation: in the absence of cracks, it delays the transport of chlorides to the reinforcement bars through the pores. In the presence of cracks, it restricts the flow of oxygen to the cathodic area, thus decreasing the corrosion rate [91]. In light of this, the use of performance-based limiting crack widths in future codes has been advocated by many researchers [92], [93]. These crack width limits should be sensitive to corrosion-affecting parameters such as cover depth and concrete quality.

Even in the case of transverse cracks, other characteristics are likely to influence their relevance in term of promoting corrosion damages. The presence of defects and

other weaknesses in the concrete may, in fact, have a greater influence [94]. Self-healing can increase a crack resistance to chloride ingress [29], while the influence of transverse cracks has been observed to be greater in dynamically loaded specimens [95]. Increased crack frequency was observed to reduce the local corrosion rate, while the influence of transverse cracks themselves was observed to decrease with the exposure time [96].

Non-destructive methods for corrosion studying and monitoring

As the reinforcement bars are embedded in concrete, it is particularly hard to observe the evolution of the corrosion process without damaging the concrete. Two different trends can be recognised in literature: one, aims at developing more accurate models, able to capture the entire corrosion process and therefore predict the service life of the structure, possibly without the support of destructive tests and field analyses. A second consists in developing non-destructive techniques, able to monitor the corrosion process. Non-destructive techniques are however essential to both trends, either to increase understanding of the parameters the predictive models are based on, or to assess the corrosion status of the structure. Examples of such methods are neutron tomography, X-ray CT, acoustic emissions, and electrochemical techniques. Some of these techniques, such as neutron tomography and X-ray CT, are mostly fit for laboratory tests, while acoustic emissions and electrochemical techniques could as well be used for field monitoring.

Neutron tomography is particularly of interest for the study of the corrosion process, since neutrons have high hydrogen-sensitivity. Corrosion products are in fact a combination of iron, oxygen and hydrogen and have a high attenuation value using neutron tomography, i.e. they are easy to identify. The use of neutron imaging to study concrete is rather recent, but several applications have already been shown [97]–[100]. The use of neutron imaging for the observation of corrosion in concrete has however been attempted only once to the author´s knowledge before the current work [101]. X-ray tomography is another imaging method, but is quicker and more broadly available than neutron imaging. X-ray CT has already been used to observe corrosion products with various degrees of success in previous studies [80], [102]. X-ray attenuation values change with the density of the substance: hydrogen is almost transparent to X-ray, while iron is strongly attenuating. Hence, observing, and especially quantifying corrosion products in a normally sized reinforcement bar can be somehow difficult, but in recent work, new techniques and algorithms have allowed for improved recognition of different phases in un-reinforced concrete through X-ray CT [97].

Acoustic emissions and electrochemical techniques are examples of non-destructive

methods more oriented towards field monitoring. Acoustic emission (AE) is a passive method that monitors the transient stress waves generated by the rapid release of energy from localized sources, e.g. fracture. The method can be used to monitor the evolution of local damage in concrete structure, particularly to monitor degradation induced by corrosion [103]. Acoustic emissions analyses have been utilized in combination with micro-CT to successfully quantify and locate the amount of corrosion damage in small scale samples[104]–[107].

Non-destructive, electrochemical methods for the assessment of corrosion in concrete were already in use in the 1970s, with the measurement of corrosion potential. In the following years, methods to monitor resistivity, galvanic current, oxygen limiting current and chloride content where introduced. Electrochemical methods can either be used as embedded sensor, put in place at the time of casting of the structure, or for routine monitoring. Common methods are:

- Open circuit potential (OCP), which measures potential in relation to a reference electrode, and indicates either a low or high probability of corrosion occurrence;
- Resistivity measurements, which capture the ability of the concrete to carry electrical current. A trend of decreasing corrosion rate with increasing concrete resistivity is often reported in literature, but its accuracy is somehow controversial [40];
- Polarization resistance, where corrosion rate is determined by applying a small known potential or current value to the reinforcing steel and monitoring current or potential variation for a certain period of time.

Studies on non-destructive methods are currently the object of large recent efforts, and new techniques are being developed.

CHAPTER 3

Bond of naturally corroded, plain bars

"The story so far:
in the beginning, corrosion was created.
This has made a lot of people very angry
and been widely regarded as a bad move."
(Adapted from The Restaurant at the End of the Universe [108])

The first research question addressed in this thesis looks into how natural corrosion influences the bond and anchorage of plain reinforcement bars. This was done by testing and later analysing the results of structural tests carried out on specimens sourced from a decommissioned bridge in Sweden (Gullspång bridge). The work related to the first research question was conducted through two experimental programs, 3-point bending tests (*Paper B*) and pull-out tests (*Paper C*), and a study on the structural behaviour of the 3-point-bending tests, carried out with finite element analyses (*Paper D*). This chapter opens with an overview of Gullspång bridge and the material characteristics of the edge beams, followed by an introduction to the studies listed above and a summary of the main results obtained from each study.

3.1 Gullspång bridge

The edge beams of Gullspång bridge were donated to Chalmers to be used to test and obtain data on the anchorage and bond-slip behaviour of naturally corroded, plain reinforcement bars. Later on, parts of the structure was as well used in the third experimental program (see Chapter 4), i.e. the study of the properties of corrosion products in naturally corroded structures using X-ray and neutron tomographic data.

Gullspång bridge (Fig.3.1) was built in 1935 and torn down in 2016 due to heavy corrosion damages. The edge beams were carefully taken out, cut in segments and designated to be used for research. Having been exposed for 81 years to weather conditions that include snow, freezing-thawing cycles and wind, as well as to de-icing salts and traffic loads, the beams presented different cracks on their surface, and spalling strongly affected the geometry in some locations (Fig.3.1). Signs of corrosion were clearly visible, but not uniformly distributed.

Figure 3.1: Gullspång bridge: view of the bridge before demolition (left) and exposed tensile reinforcement bars and spalling in an edge beam (right). Photos courtesy of Ignasi Fernandez

Geometry and material properties

The edge beams were characterized by ϕ6 stirrups, open on the bottom side with respect to the original position on the bridge and 2ϕ16 plain reinforcement bars, top and bottom (Fig.3.2). The concrete cover varied approximately between 20 and 55 mm, but was reported equal to 34 mm in the original drawings. Average cross-section dimensions were 300 mm x 250 mm. All specimens contained approximately a 50 mm part of the slab deck. Spacing of the stirrups ranged between 100 and 450 mm, in contrast to the typical 300 mm spacing referenced on the drawings.

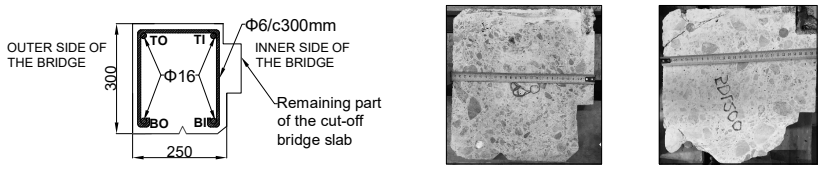

Figure 3.2: Edge beams cross-section geometry (according to the original drawings) is shown on the left. Photographs of two cross-sections are shown on the right. Bar naming convention is as follows: TO= Top-Outer, TI= Top-Inner, BO= Bottom-Outer and BI= Bottom-Inner. The remaining part of the slab-deck is clearly visible to the right. All dimensions are in mm.

In Table 3.1 an overview of the main material properties of concrete and steel reinforcements in the edge beams is given, as obtained from material tests carried out in this project. The original drawings cited an average concrete compressive strength of 30 MPa and a nominal yield strength of reinforcements of 300 MPa. This information is however not consistent with the results of the material tests shown in Table 3.1. The increased compressive capacity of the concrete is however consistent with the age of the bridge. More information on the material tests can be found in *Paper B*, except for the characterization of tensile strength and fracture energy, which was obtained at a later time, in connection with a project aimed at recycling the concrete from the specimens used for the 3-point-bending tests.

Tensile strength and fracture energy were obtained from four cores (100 mm x 100 mm) tested in uniaxial tension. The value obtained for the fracture energy, however, was observed to be significantly larger than the fracture energy estimated from the calibration of the FE analyses in *Paper D* (approximately one third of the value obtained in the tests, 90 Nm/m^2). The large size of some aggregates can likely explain this difference, since large aggregates were observed in all of the tested cores.

Large aggregates, with a diameter often exceeding 16 mm, are not uncommon in concrete structures from the 30s. The concrete was as well tamped instead of being vibrated, as it is common today: this might have increased the presence of voids and the size of the bleeding zone. Additionally, during the investigation with X-rays and neutron tomography, the presence of a small amount of scandium (Sc) was reveled in the cement paste by a neutron spectroscopy of the sample. The element, classified as a rare-earth material, is rarely present in concrete, but gave unexpected problems during neutron scanning, since one of its isotopes has a half-life of 83.8 days. The reinforcement bar type and quality reflected as well common practice at time of

Table 3.1: Material properties of the edge beams of Gullspång bridge

Concrete	
Compressive strength $[MPa]$	45.6±4.6
E modulus $[GPa]$	27.4±3.3
Tensile strength $[MPa]$	2.9±0.53
Fracture energy $[Nm/m^2]$	230±54
Reinforcement bars	
Yield strength $[MPa]$	259.6±10.1
Cross sectional area $[mm^2]$	204.5±0.97

construction. Bars were generally of lower capacity and more ductile compared to the modern counterparts, and anchorage was assured through use of end-hooks.

Test preparation

All specimens underwent visual inspection prior to testing, to document exact measurements of the cross-section geometry, locations, and width of existing cracks. The average opening of the cracks was measured with an optical microscope and their location and length were documented and photographed. Data on cracks was used to group the anchorage zones into three different categories (see Fig. 3.3): anchorage zones with cracks smaller than 0.5 mm (C1), anchorage zones with cracks between 0.5 and 1 mm (C2), and anchorage zones with cracks with more than 1 mm of average opening (C3). Additional categories, 'reference' (R) and 'severely damaged' (S) were added to provide low and upper bound groupings of damage state.

The preparation for the planned tests required cutting off segments of the edge beams in different lengths (*Paper B* and *Paper C*), and drilling of cores for material testing and for imaging (*Paper E*).

Initially, the edge beams were carefully taken out and cut in 2 to 6 m segments at the demolition site, to allow for transportation. In Figure 3.4, the layout of the edge beams is presented. Each segment was assigned a number on site, to allow for locating its original position on the bridge. The segments were later cut in smaller pieces, with different thicknesses (90 cm for the beam tests, and 5, 7.5 and 10 cm for

(a) reference 'R'

(b) cracks<0.5 mm 'C1'

(c) 0.5≤ cracks<1 mm 'C2'

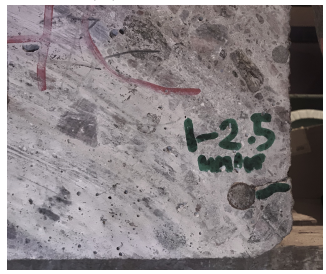

(d) cracks≥ 1 mm 'C3'

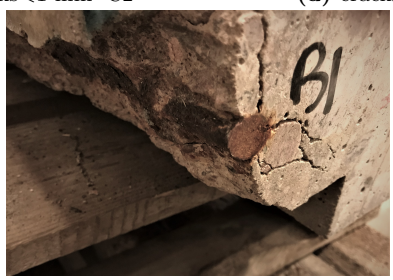

(e) severely damaged 'S'

Figure 3.3: Examples of test specimens categorised according to their varying deterioration states.

the pull-out tests) to fit the design of the experimental program. Letters were used to denote the specimens resulting from these later cuts, in addition to the original position. The cutting was carried out with all the segment oriented in the same direction: this implies that the specimens from the west edge beams were named in alphabetical order from north to south, while the specimens from the east edge beam followed the alphabetical order from south to north.

A core was as well taken from the edge beams for the imaging study. The sample was drilled from a specimen initially designed for pull-out testing (75 mm thickness), using a water-cooled drill, and by keeping the speed of the cutting to a minimum to avoid damaging the specimen.

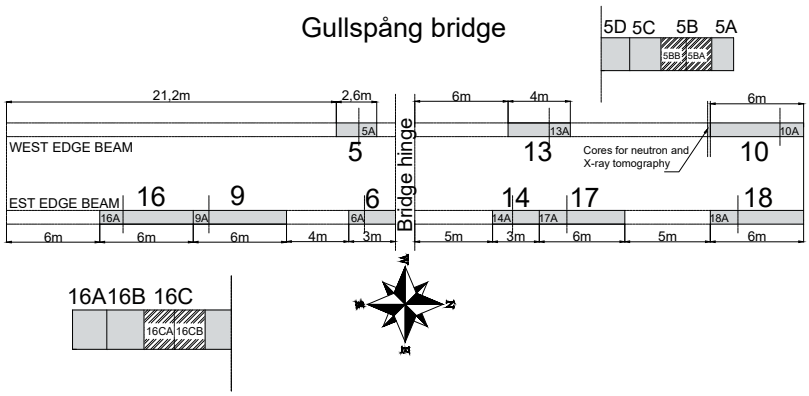

Figure 3.4: Original position of the segments extracted from Gullspång bridge.

Designing of the test setups

Testing specimens taken from a decommissioned structures presented some challenges. Test set-ups needed to be designed to adapt to the given material and geometrical properties. Any modification risked damaging the specimens and needed to be done carefully. Another complication was that the geometrical properties, such as concrete cover and stirrup spacing, varied from specimen to specimen. Appropriate, non-destructive methods to investigate the characteristics of each specimen were as well needed before proceeding with cutting. Design of the test set-ups was divided in four main phases:

- Phase 1: a study was conducted into available literature. Finite element (FE) modeling was employed to assess possible set-up configurations, and different testing methodologies were selected from literature;
- Phase 2: prospective test configurations were tested in-lab as part of pilot investigations;
- Phase 3: the test set-ups for the experimental programs were chosen by analysing and comparing the results of the pilot studies.
- Phase 4: complementary material tests were selected.

3.2 Three-point-bending tests

The first experimental program was designed to test and obtain data on the anchorage of naturally corroded, plain reinforcement bars. Specifically, based on an extensive literature review, the following points were highlighted as important to be included in the study:

- Bottom-cast and top-cast bars were observed to have different bond characteristics in several studies, both corroded and uncorroded, due to differences in the density of concrete surrounding the bars. The tests were therefore designed to investigate the anchorage of bottom and top-cast bars;
- The presence of corrosion-induced cracks and/or spalling was a second factor likely to influence anchorage capacity, therefore cracked and uncracked conditions of the concrete surrounding the reinforcement bar needed to be included in the test;

Additionally, the following general design requirements were established for the test-set up:

- The test set-up needed to have a high chance to reach anchorage failure;
- The test set-up needed to be simple and easy to carry out without need for strengthening of the specimen;
- The slip of the tensile bars during the test needed to be tracked;
- The tensile reinforcement bars, and specifically the steel-concrete interface, were to be disturbed as little as possible;
- The test set-up needed to allow for testing both bottom-cast and top-cast bars.
- External confinement was to be reduced to a minimum, since the use of direct supports was likely to increase the anchorage capacity of the bars, by increasing normal pressure.

Description of experiments

The final test-set up was selected following a pilot study, where two 4-point bending tests and a 3-point bending test were tested. Descriptions and details of the pilot testing is given in *Paper A*. A directly supported 3-point bending test was selected to provide the best collection of results, owing to the simplicity of the test set-up and the well defined crack pattern, characterized by a single bending crack underneath the load plate. The 4-point bending test was not selected due to higher uncertainties in the crack pattern.

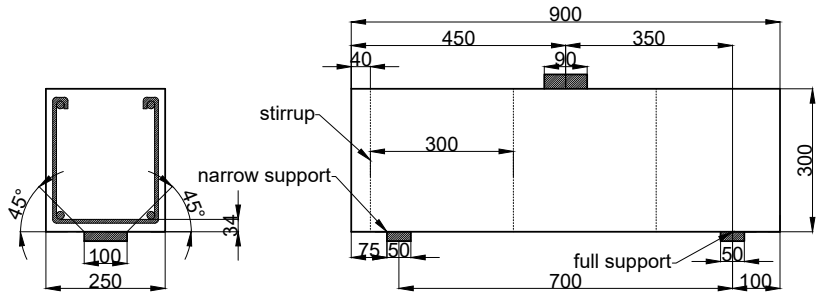

Figure 3.5: Experimental set-up and view of the narrow support for a beam tested upside-down compared to its position on the bridge.

Twenty beam specimens were tested. Figure 3.5 gives details on the beam geometry and the 3-point bending test configuration.

The tested beams were 900 mm long, with a theoretical span of 700 mm. They were supported on one side by a narrow support (50 mm x 100 mm) and a full support (50 mm x 250mm) on the opposite side. Both the load plate and the two supports consisted of a steel block and a thin wood-fibre layer inserted between steel and concrete. The aim of the narrow support was to minimize the effect of support pressure. To meet this objective, a smaller support plate was positioned in the middle of the beam (between the bars) and specifically located on the side expected to have anchorage failure. The specimen was specifically cut to have a stirrup external to the narrow support to help redistribute the higher concentrated stresses generated by the support. On the opposite end, at the location of the full support, the ends of the reinforcing bars were restrained from anchorage failure by means of a bolt/washer configuration. However, out of the first four tests, two beams showed bending of the washers and unwanted slipping of the restrained tensile reinforcements. It was opted not to restrained the reinforcement bars, but to monitor the end-slip on both sides for subsequent beams. This behaviour, initially unexpected, was further clarified by the Non Linear Analyses carried out in *Paper D*, where an asymmetric behaviour of the yield penetration was observed in the tested beams. This asymmetry is likely due to differences in the bond conditions between the right and left side of the beam. The use of bolt and washers lead to an increase in the asymmetry in the bond behaviour of the bar.

Summary of the results

The tests were characterized by the opening of one or two major bending cracks, that was closely followed by yielding of the tensile reinforcements. In most of the tested beams, their load-carrying capacity was limited by yielding of the bars. Slipping of the tensile reinforcement took place after yielding of the tensile reinforcements. The beams failed in bending: slipping of the bars occurred at a point where the bending cracks had already reached an opening width of several centimetres. In Fig. 3.6 load-displacements curves for each tested specimen are presented. In Fig.3.7, the typical crack patterns exhibited by the specimens are shown.

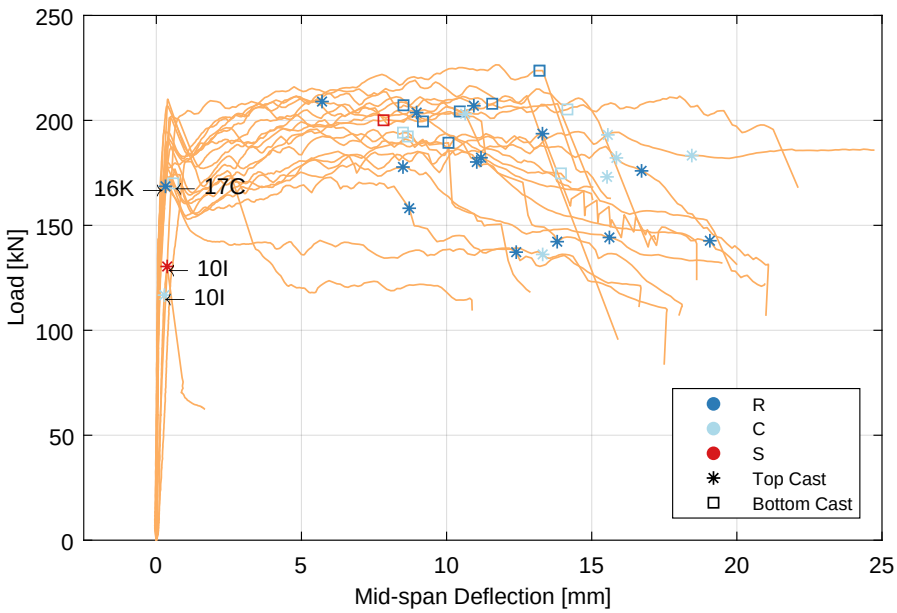

Figure 3.6: Load-mid-span deflection curves for the three-point bending tests. The markers show where each bar started to slip; colours indicate the level of damage in the anchorage zone. The impact of the cast position is shown by an asterisk for the top-cast bars and by a square for the bottom-cast bars. The labels of the beams where end-slip of one or more bars took place without yielding are marked.

Yielding of the reinforcement bars was a necessary feature of the structural tests, due to the high cracking and low bending moment in the cross section of the beams. Yielding of the reinforcement bars took place in all but one of the 20 beams tested,

the low yield strength of the tensile reinforcement resulting in the bars reaching yield stress near the time of opening of the first bending crack.

The loss of bond at yielding was an important factor in defying the structural behaviour of the beams. The low bond stress along the yielded length changed this behaviour from beam to arch action: the low bond stress in the yielded part of the bar resulted in the stress in the bar being almost constant along the length, changing the position of the lever arm instead. The low bond resulted as well in an increased transferring length so that, after the opening of the first bending crack, the bond between steel and concrete could not transfer enough stresses to the concrete so that it would exceed its tensile capacity and form another bending crack. At the same time, the yield penetration continued to increase.

The use of 3D scanning techniques allowed for an in-depth study of the behaviour of the reinforcement bars. Yield penetration and corrosion damages were easy to identify by 3D scanning, and the average anchorage capacity was estimated both in the unyielded zone, but also in the yielded zone.

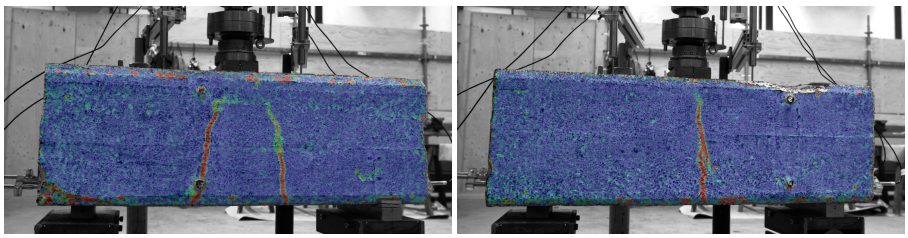

Figure 3.7: Beam 17H (Left) and Beam 9B (Right): example of typical crack patterns, as captured by Digital Image Correlation (DIC) cameras.

The average anchorage strength of the unyielded zone was estimated to a value (7.39 MPa) that was more than double what reported in previous literature: different casting techniques, the effect of natural corrosion, and the difference in surface roughness of the steel bars are possible factors explaining such differences.

Moreover, the tests were able to confirm the expected influence of the casting position (see Fig. 3.8). When uncorroded, bottom-cast bars had a higher anchorage strength than that of top-cast bars. Corrosion decreased the bond strength of bottom-cast bars and led to the opening of spalling cracks. Small corrosion levels increased the bond strength for top-cast bars. Additional information can be found in *Paper B*.

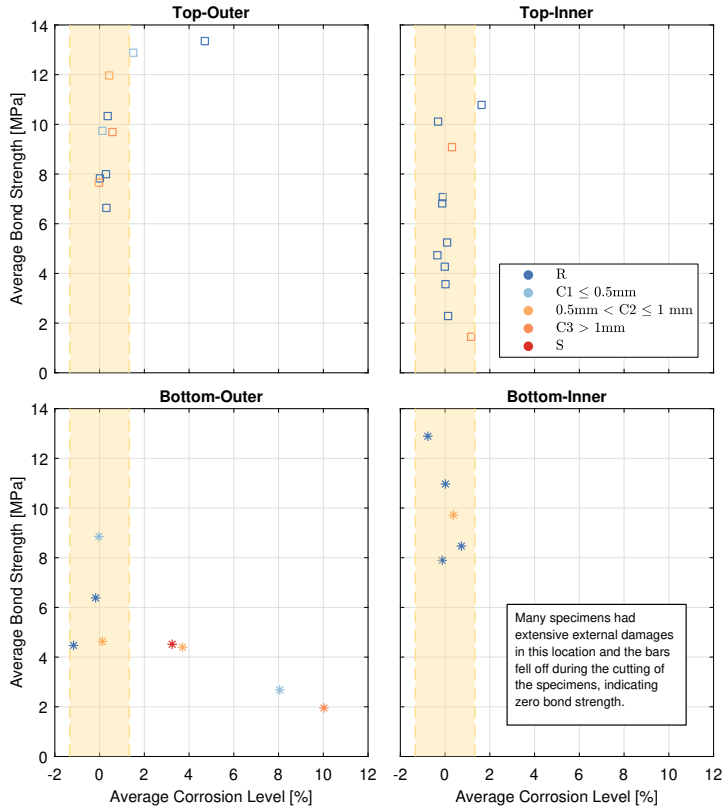

Figure 3.8: Plot of the average bond strength in the unyielded zone against the average corrosion level. Different colours are used to indicate the level of damage in the anchorage zone. Results from different positions in the cross section are displayed separately: top-outer (left, top), top-inner (right, top), bottom-outer (bottom, left), and bottom-inner (bottom, right). The shaded area represents the accuracy in the evaluation of the corrosion level at zero, due to the uncertainties in the reference area of the uncorroded bars

3.3 Pull-out tests

The second experimental program included 156 pull-out tests of reinforcement bars with an embedded length of 50, 75 and 100 mm. The program was design to investigate the bond-slip behaviour of corroded plain bars, and specifically the test set-up was chosen based on the following:

- The test set-up needed to fully capture the bond-slip behaviour of the bars, including the post-peak behaviour;
- Passive and active slip needed to be recorded;
- Yielding of the reinforcement bars was to be avoided;
- The test set-up needed to be quick and easy to reproduce, allowing for a large number of tests;
- The specimens needed to be designed and chosen so that some would include stirrups, and some not;
- The specimens needed to include different levels of damage in the surrounding concrete.

Description of experiments

Direct pull-out tests were performed using cut sections (50, 75 and 100 mm in thickness) from untested segments of the edge beams from Gullspång bridge. The length of the reinforcement bars was designed to avoid reaching the yield point. The need of avoiding yielding of bars gave an upper limit of 100 mm embedded length. The lower limit was set to 50 mm, for feasible cutting of concrete slices and drilling (20 mm deep) not to affect the major part of the length.

The test set-up required drilling, threading, and inserting a threaded rod in the individual reinforcing bars. Thereafter, each individual bar was pulled out using a hydraulic load cell. A special rig was designed and produced in-house (see Fig. 3.9). This consisted of three legs, two of which could be length-adjusted to account for any skew angle between bar and cut concrete surface.

There was a total of 174 bars, of which 104 were in concrete without visible damage, 35 had cracks, and 35 had some spalling of the concrete cover. Additionally, 30 tested bars had a stirrup embedded in the surrounding concrete.

Summary of the results

Of the 174 bars available for testing, 156 were successfully tested during the experimental program. The results had a large scatter, but some trends were clearly visible. First, the casting position had a significant influence on the bond behaviour,

Figure 3.9: Photographs of pull-out rig and slip measurement devices. Note that specimen to the right is tilted with respect to normal testing position to better show the measurement device.

as observed as well in the previous tests. Additionally, as shown in Fig. 3.10, the corrosion level necessary to damage the surrounding concrete was observed to be smaller for bottom-cast bars than for top-cast bars. This is likely a consequence of the concrete density variation.

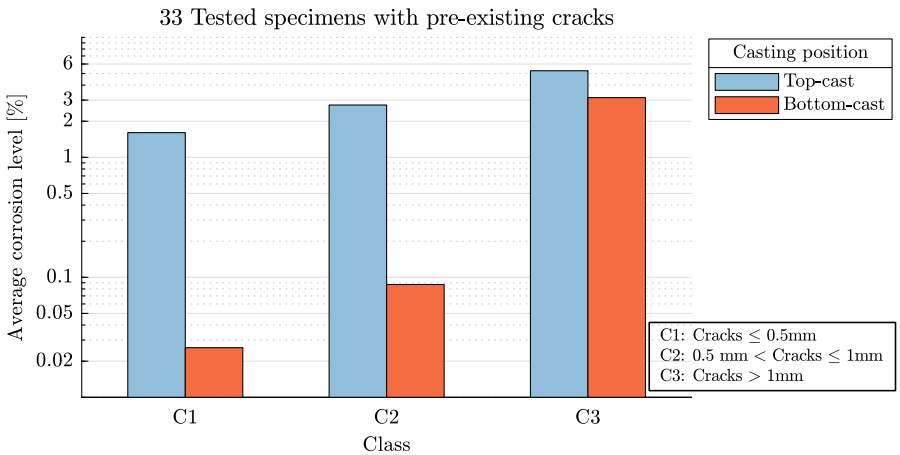

Figure 3.10: Average corrosion level of specimens with cracks in the surrounding concrete, sorted by crack width. Note that the y-axis is in logarithmic scale.

The test set-up allowed as well to look into the effect of stirrups on the bond of corroded plain bars. In Fig. 3.11, the residual bond strength is plotted against the

peak-bond strength. The presence of a stirrup is shown to positively impact the residual bond stress capacity regardless of the damage level of the specimen. The stirrup also contributed to maintaining the bond strength in specimens presenting several cracks, spalling, or large crack openings.

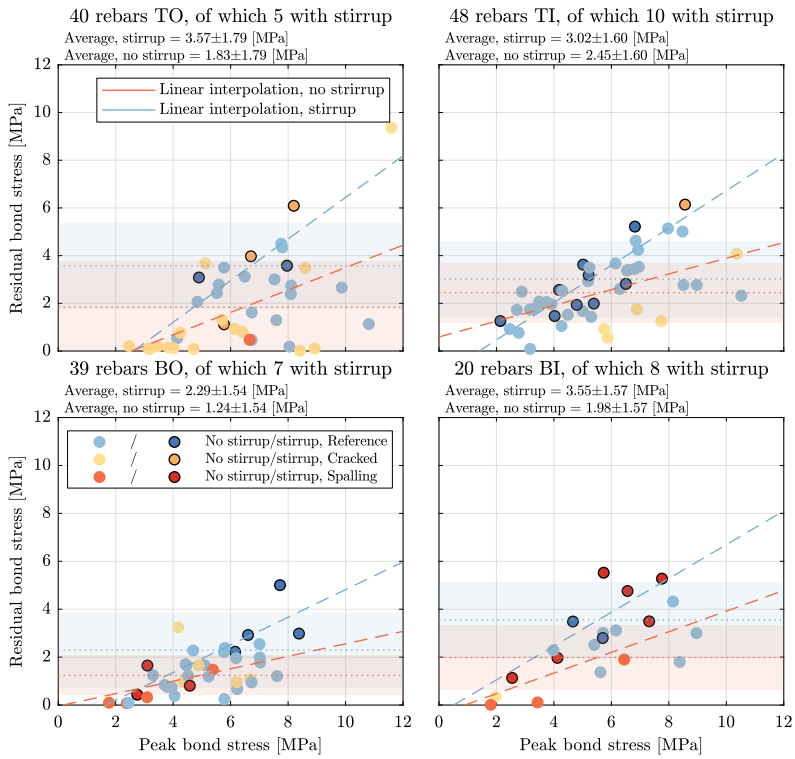

Figure 3.11: Residual bond stress vs. peak bond stress. Specimens are divided by casting position. Two different linear fits are presented per graph: in blue, specimens with a stirrup, in red, specimens without a stirrup.

In Fig. 3.12, the peak bond strength obtained from the 3-point-bending tests and pull-out tests is plotted against the average corrosion level. Results from top-cast bars and bottom-cast bars are plotted separately. The peak bond strengths in the two tests are in good agreement, both for top- and bottom-cast bars. However,

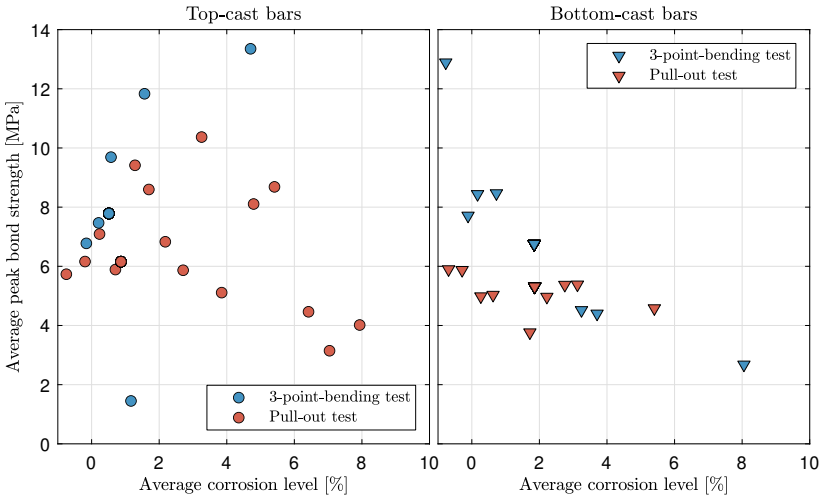

Figure 3.12: Average peak bond strength and corresponding average corrosion level of top- and bottom–cast bars tested both in 3-point bending and with pull-out tests. Each point in the graph represents the bond strength of the tested bars averaged over an interval of 0.5% of corrosion.

the average peak bond strength recorded in the pull-out tests is consistently lower than in the 3-point bending tests. This may be due to the contribution of support pressure in the anchorage zone in the 3-point bending tests.

3.4 Finite element analyses

The bond behaviour of the plain bars in the 3-point bending tests could not be completely defined only with the experimental data collected. Particularly, it was not possible to define the residual bond strength, though it was evident in the tests that this bond contributed to the load carrying capacity of the beam after the first bar started slipping. The loss of bond at yielding was as well only estimated for a few bars. It was therefore decided to run finite element analyses calibrated on the experimental results to try to capture the missing aspects of the bond behaviour. Additionally, the analyses offered the opportunity to look into the structural effects of the long, asymmetric yield penetration along the length of the bars developed in the tested beams. The results of this analyses are presented in *Paper D*.

Description of the analyses

The structural behaviour of 9 of the beams tested in *Paper B* was modelled using non-linear finite element analyses, using the commercial software Diana 10.2 [109]. 1D bond-slip relationships were used to represent the bond between the naturally corroded plain bars and the concrete. Each bar was divided in three different zones according to test measurements: two unyielded zones and one yielded zone (see Fig. 3.13). The yielded zone corresponded to the yielded zone along the length of the bar at the end of the structural test.

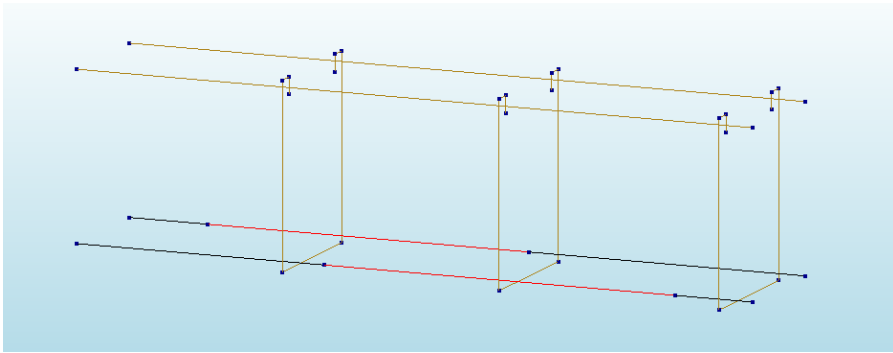

Figure 3.13: Layout of reinforcement bars, showing the division in yielded (in red) and unyielded zones (in black) in finite element analyses. The brown-marked reinforcement was modelled assuming full interaction to the concrete.

Two bond-slips relationships were defined, one for the unyielded and one for the yielded zones (see Fig. 3.14). A total of 9 parameters of the bond-slip curves were calibrated for each bar, representing various stresses and slip value in the bond-slip curves. The curves were calibrated iteratively by comparing the results of the finite element analyses with the experimental data. Particularly, the compared aspects were: load-deflection, crack pattern, crack width, yield penetration along the length of the bar and asymmetry in yield penetration length.

Summary of the results

The study highlighted the importance of including the loss of bond at yielding and the asymmetry of the yield penetration in the finite element analyses to describe the structural behaviour adequately. The asymmetry of the yield penetration caused one of the sides of the beam to have a shorter available anchorage length and thus,

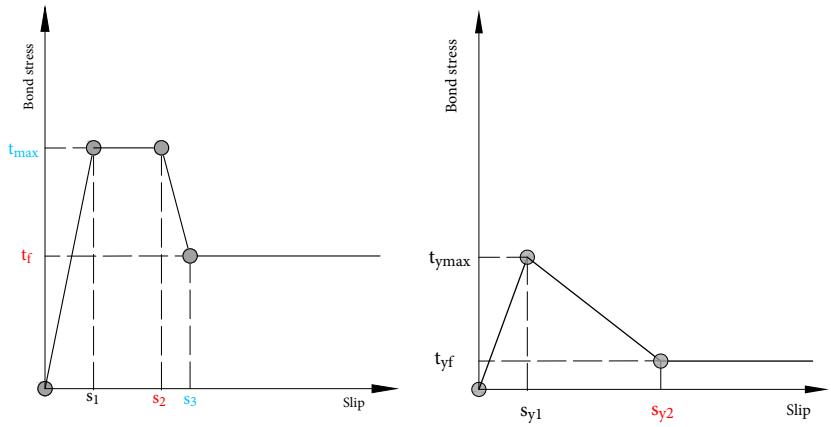

Figure 3.14: Bond-slip relationships for (a) unyielded zones and (b) yielded zone. The parameters are divided into three sets: 1 (black), with the same values for all bars; 2 (blue) calculated manually and 3 (red) calibrated individually.

governed the anchorage failure mode. It is nowadays common to utilize symmetries in a structure to reduce computational cost, but, given the observed behaviour, it could lead to a significant overestimation of the anchorage length.

Additionally, the study, by calibrating the bond-slip curves, allowed for an estimation of the residual bond strength in the three-point bending tests. In Fig. 3.15, the residual bond strength is plotted against the maximum bond strength, as obtained from the calibration of the bond-slip curves. The residual bond strength recorded in the pull-out tests (defined as the bond stress recorded at 4.5 mm of slip) is as well plotted against the maximum recorded bond strength. The presented results are for top-cast bars, given the limited amount of bottom-cast bars included in the finite element study. Pull-out tests and calibrated FE analysis results of the beams show good agreement, both in magnitude and in trend. This is particularly of interest, since residual bond strength is hard to define experimentally from 3-point bending tests, but easy to obtain with pull-out tests.

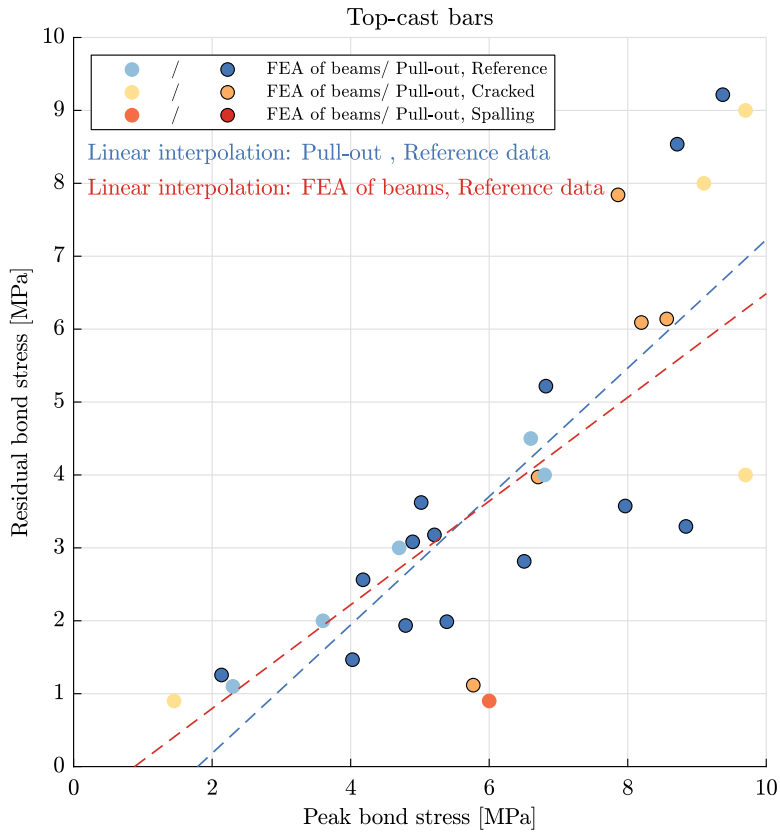

Figure 3.15: Residual bond stress versus the maximum bond stress of top-cast bars, as obtained from the calibration of FE analyses of beams and pull-out test results. Results from reference specimens are linearly interpolated, for FE analysis (in orange), and for pull-out tests results (in blue). Different colours of the markers indicate different levels of damage in the surrounding concrete.

CHAPTER 4

Characteristics of the corrosion products and the surrounding concrete

"In a hole in the bar
there lived corrosion products."
(Adapted from The Hobbit [110])

The second research question looks into the characteristics of the corrosion products and the surrounding concrete that are relevant to assess and predict corrosion damages in existing structures. Particularly, it focused on those characteristics important for modelling the corrosion cracking process and it was deemed important to select non-destructive methods for the investigation. The study aimed, additionally, at looking into the differences between natural and artificially corroded samples.

An experimental program was designed to address these questions. The program comprised the acquisitions of neutron and X-ray tomographic data from two concrete cores, of which one extracted from Gullspång bridge, and one lab-made and artificially corroded via the galvanostatic method (*Paper E*).

Neutron imaging and X-ray tomography were selected as non-destructive methods. Neutron imaging was selected due to the high hydrogen-sensitivity of neutrons, which made it particularly fit for detecting and quantifying corrosion products. Then, the instrument D50 at the Institut Laue-Langevin (ILL) in Grenoble provided the op-

portunity to use both neutron and X-ray tomography. The instrument allows, in fact, for performing both image acquisitions in the same experimental set-up, one after the other. The use of multiple imaging techniques is known as multimodal imaging, and it takes advantage of the high complementarity in the attenuation mechanisms that neutrons and X-rays have when interacting with reinforced concrete. By combining data obtained with both methods, it allows an easier, and more precise identification procedure for the different phases contained in the sample.

Finally, it needs to be added that although in this work only two samples were studied, one naturally corroded and one artificially corroded, data from additional cores was acquired at the time of scanning. The experimental campaign was aimed at looking at the feasibility of using neutron and X-ray tomography to acquire information on corrosion products and their distribution, and lays the groundwork for future, planned studies, where data is to be acquired to calibrate corrosion models for capturing different aspects of the corrosion process.

4.1 Description of experiments

Two concrete cores were studied by neutron and X-ray tomography (See Fig. 4.1). One core was taken from the edge beam of Gullspång bridge. The core was 50 mm long, had a diameter of 25 mm, and contained a top-cast plain reinforcing bar with a diameter of 16 mm. The analysed sample was uncracked and its material characteristics can be found in Table 3.1.

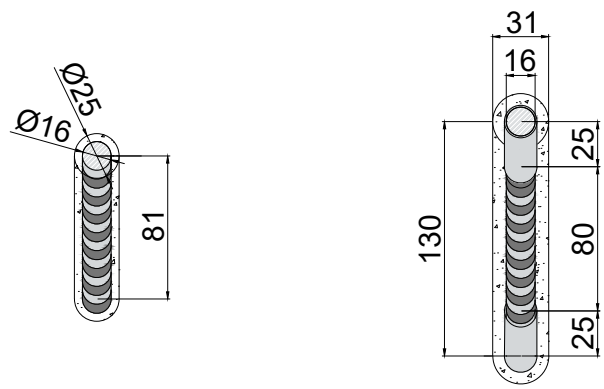

Figure 4.1: Geometry of natural (left) and artificial (right) corroded sample. All measures in mm.

The artificially corroded sample was prepared in the laboratory, adopting a plain

reinforcing bar with a nominal diameter of 16 mm extracted from the edge beams of Gullspång bridge. The bar was sandblasted before casting. The bar was positioned in the middle of a 130 × 150 mm concrete cylinder, and embedded in the concrete cylinder for a length of 80, while plastic holders (25 mm each) were used to cover the top and bottom parts of the bar. The cylinder was cast standing on its base with the reinforcing bar (which had a total length of approximately 200 mm) protruding from the top. Additional information is available in *Paper D*.

The neutron and X-rays tomographic data was obtained at the instrument D50 at the Institut Laue-Langevin (ILL) in Grenoble. The acquired radiographies were reconstructed into the corresponding 3D volumes with the commercial soft-ware X-act (from RX-Solutions). The resulting images have a pixel size of 26 μm/px for the neutron data, and of 36 μm/px for the X-rays data.

4.2 Summary of the results

Multimodal neutron and X-ray computed tomography was used to obtain qualitative and quantitative data on the characteristics and distribution of the corrosion products in the samples. Neutron and X-rays data were aligned and superimposed, thus allowing for recognizing different phases in the studied specimens, including corrosion products. In Fig.4.2, the output of the phase segmentation for a cross-section of each sample is shown. Five components are identified for each sample: reinforcement bar, cement paste, aggregates, voids and corrosion products.

Fig. 4.3 shows the corrosion distribution in the two samples, as obtained after post-processing of the acquired data. The corrosion products appear to be differently distributed in the artificially and in the naturally corroded sample: the products adhere to and are diffused through the cement paste for the case of the artificially corroded sample, while they adhere to the bar in the naturally corroded sample. Additionally, in the naturally corroded sample, corrosion products are to be found in correspondence of large voids at the steel-concrete interface. This voids are consistently present on one side of the bar, which was identified as the bleeding zone resulting from the top-cast position of the analysed bar. Corrosion products were instead approximately uniformly distributed in the artificially corroded sample.

Most importantly, key metrics for the modelling of the corrosion process were observed, and it was possible to measure the thickness of the corrosion products at the steel-concrete interface, and the iron-to-rust ratio.

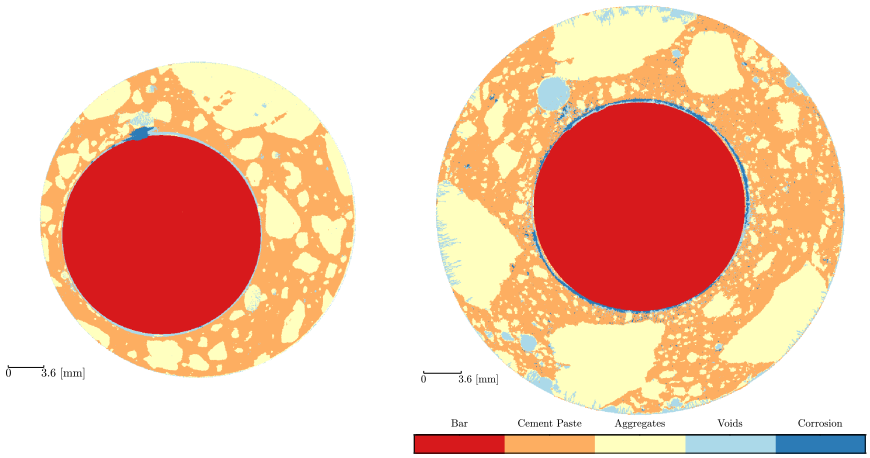

Figure 4.2: Phase segmentation of the samples. Cross-sections of the naturally corroded sample (left) and the artificially corroded sample (right) are shown.

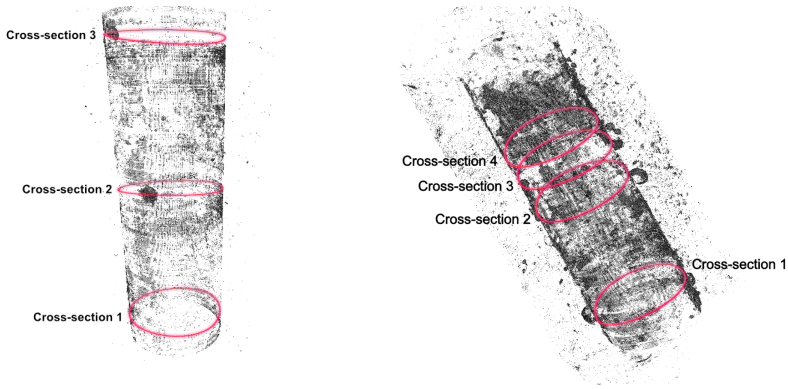

Figure 4.3: 3D rendering of the corrosion distribution around the bar for the naturally corroded sample (left) and the artificially corroded sample (right).

CHAPTER 5

Impact of transversal cracks on corrosion characteristics

"The two cracks appeared out of nowhere,
a few decimeters apart in the narrow, concrete beam."
(Adapted from Harry Potter and the Deathly Hallows [111])

The third research question focuses on load-induced transversal cracks in reinforced concrete structures exposed to chloride environments. The surface crack width of load-induced cracks is strictly regulated in codes as a way to ensure a desired structural behaviour over time, specifically, as a way to prevent and/or delay corrosion damages. The work aimed at looking in a systematic way to the effect of transversal cracks on the characteristics and distribution of corrosion damages. This was done, initially, by formulating a list of hypotheses based on an extensive literature review. These hypotheses were then tested on a dataset, compiled from data available in literature. Statistical methods were used to test the hypotheses on the collected dataset. The results of this study are described in details in *PaperF*.

5.1 Description of the study

The study identified five hypotheses, which were aimed at investigating the effect of transversal cracks on the distribution and characteristics of corrosion damages in

reinforced concrete structures exposed to chloride environments:

- **H1 (Crack and pit location)**: in the presence of transversal cracks, corrosion pits are more likely to form in the proximity of a crack.
- **H2 (Crack width and corrosion rate)**: corrosion rate increases with increasing crack widths for short exposure times. For longer exposure times, crack width does not influence the corrosion rate.
- **H3 (Crack width and corrosion area)**: the extent of the corrosion area is independent from surface crack width.
- **H4 (Crack width and cover quality)**: cover quality influences the corrosion rate more than surface crack widths do.
- **H5 (Crack frequency and corrosion rate)**: Increased crack frequency (smaller crack distances) reduces local corrosion rate.

These hypotheses were tested on a dataset containing 62 reinforced concrete specimens, tested in 3-point bending and then exposed in an environment containing chlorides for a period of time varying between 18 and 324 months. In Fig. 5.1, an overview of the dataset is presented.

The availability of data in literature limited the scope of the study to specimens exposed to de-icing salts with bending cracks. Other types of cracks, such as those due to restrains, shrinkage, temperature or pure tension have different morphology. Specifically, the width of the crack decreases with the closeness to the reinforcement bars for the case of bending cracks. Therefore, observations based on surface crack width may not be applicable to different kinds of cracks. Additionally, marine water contains other substances that may influence the penetration of chlorides through the cracks, such as magnesium.

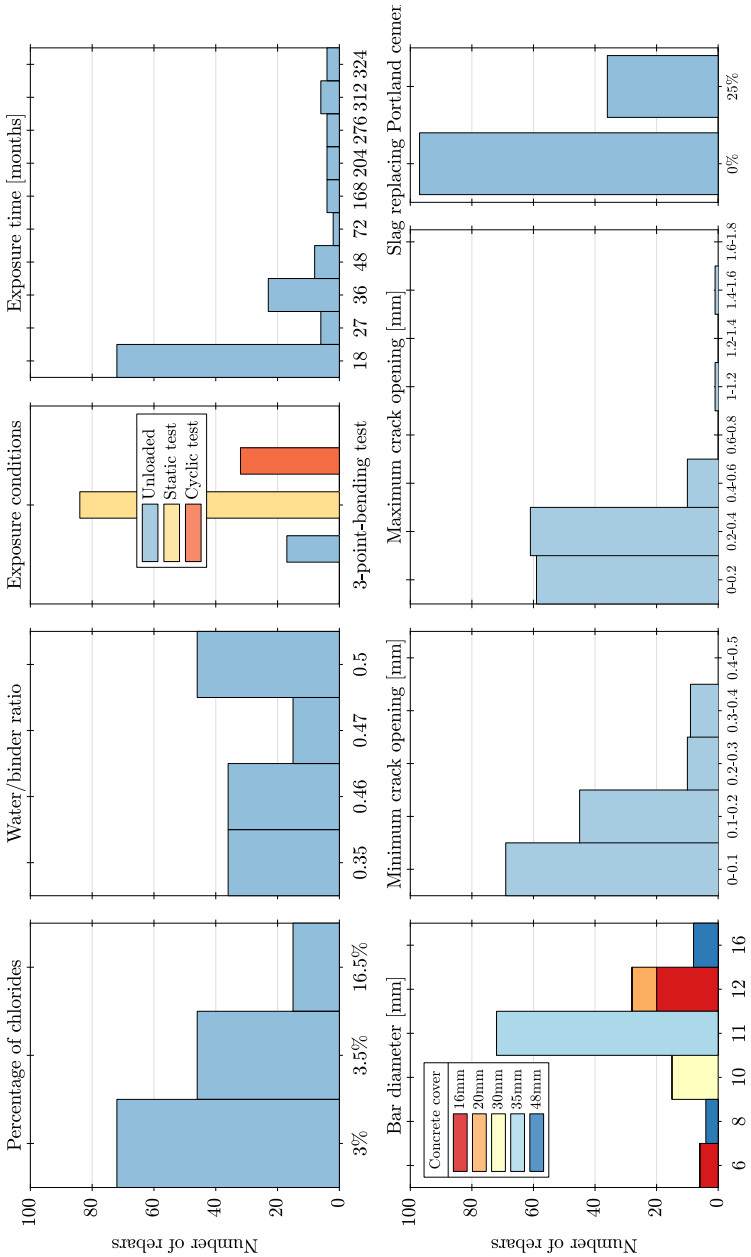

Figure 5.1: Overview of the characteristics of the specimens included in the dataset.

To test the presented hypotheses, statistical methods were used: the Pearson´s correlation coefficient (r) and Spearman´s rank coefficient (ρ) were used to study the probability of a linear or monotonous relationship between the collected parameters. Both methods output a correlation coefficient for each set of parameters in the dataset: the closer this coefficient is to 1 in absolute value, the higher the likelihood of a linear (Pearson's) or monotonous (Spearman's) relation existing between the two sets of parameters. Additionally, the statistical significance of the test was calculated, expressed as a p-value between 0 and 1. The statistical significance of the test tells us if what it is observed in the sample is expected to be true in the population. The p-value is the probability of obtaining the same data in the dataset, being the null-hypothesis true in the population, i.e. the probability that the correlation observed in the dataset is a result of chance, and there is no correlation between the variables in the population.

5.2 Summary of the results

Corrosion pits were observed to be likely to form in the vicinity of a transversal crack. However, no correlation between surface crack width and corrosion rate was observed.

With regards to the five hypotheses presented in section 5.1, the following was observed:

- **H1**: corrosion pits typically appear close to the crack, and pits in proximity of the cracks were observed to have higher corrosion rates;
- **H2**: in general, no correlation between crack width and corrosion rate was observed, neither in long nor short term experiments.
- **H3**: in the dataset, smaller crack widths surprisingly correspond to longer corrosion pits. This is probably due to unintended bias in the dataset, and a weak correlation between surface crack width and slip and separation area at the steel/concrete interface. The slip and separation area is in fact influenced by other factors than surface crack width, such as loading conditions.
- **H4**: correlations between variables representing the quality of the cover (water/binder ratio and cover thickness) and corrosion rate were highly affected by biases in the dataset. Variations in cover quality highly depended from singular experimental campaigns, and varied to a large extent in exposure time. Being corrosion rate equal to the measured corrosion damage normalized by the exposure time, it was not possible to discern between the contribution of the different factors. Increasing cover thickness was however observed to decrease the amount of corrosion pits per meter of bar.

- **H5**: an increased distance between cracks was expected to result in an increase of corrosion rate at the single pit. This was as well likely to depend from the presence of biases in the dataset, specifically due to correlations between exposure time and average crack distance.

CHAPTER 6

Concluding Remarks and Future Work

It was inevitable:
the sight of chloride-contaminated concrete
always reminded him of the fate of corroded bars.
(Adapted from Love in the Time of Cholera [112])

The aim of this research was to investigate the structural effects of natural, chloride-induced corrosion in reinforced concrete structures. Within this area, three main questions were formulated. This section contains the main conclusions drawn from the work presented in this thesis. After general conclusions, main findings are presented following the order of and divided based on the research questions (see *Section 1.2*). Finally, suggestions for future research are given, based on the presented findings.

6.1 Conclusions

General conclusions

The studies presented in this work look at different aspects of natural corrosion, from its effect on the bond of plain bars, to the characteristics of the steel-concrete interface. Most of the studies make use of a decomissioned bridge (Gullspång bridge)

for studying characteristics and structural effects of natural corrosion, and highlight how using decommissioned structures allows for reaching a deeper understanding of the materials used at the time of construction and their deterioration process. Through the different studies, a comprehensive view of the corrosion damages in the 80-year-old structure was obtained, both of how they were distributed and of how they affected the structural behaviour.

The presence of a bleeding zone underneath the top-reinforcement bars, and in general, macroscopic voids at the steel-concrete interface, was observed to be of high importance. Corrosion was shown to likely initiate at the bleeding zone, where corrosion products would accumulate without inducing additional stresses on the surrounding concrete. Consequently, corrosion-induced cracks appeared in the concrete surrounding top-cast bars at a time when a significant part of the cross-sectional area was already lost. Time to corrosion-induced cracking was significantly delayed with respect to what can be inferred from experiments conducted on artificially corroded specimens, but also with respect to the bottom-cast bars of the same structure.

In the last study, the effect of load-induced transversal cracks on corrosion rate and distribution was studied. The study was based on laboratory specimens, pre-cracked and exposed to chloride solution. All data were obtained from works available in literature. The work highlighted the complexity of the corrosion process in concrete structures, together with the interrelated influence of transverse cracks with other characteristics of the concrete, such as water/binder ratio and concrete cover. Corrosion pits were observed to be likely to form in the proximity of transversal cracks.

Q1: Effect of natural corrosion on bond of plain bars

Specimens from a decomissioned bridge were taken, measured, prepared, tested and evaluated with the aim of investigating the anchorage capacity and bond of naturally corroded plain bars. The following conclusions were drawn:

- Plain bars are an old type of reinforcement bars no longer in use nowadays. The bond behaviour of plain bars is fundamentally different from the bond behaviour of deformed bars, not only given the absence of ribs, but also due to differences in the materials and overall geometrical characteristics from bars in use nowadays. The bars tested in this work had low yield strength, high ductility and were surrounded by heterogeneous concrete with large aggregates. All these characteristics are of fundamental importance when assessing old structures with plain bars.
- The presence of corrosion products affects plain reinforcement bars differently based on the density of the surrounding concrete: top-cast bars, surrounded

by less dense concrete, initially increase their peak bond strength with increasing corrosion level. Corrosion-induced cracks tend to develop later in the corrosion process for the concrete surrounding top-cast bars if compared to the concrete surrounding bottom-cast bars, possibly due to corrosion products accumulating in macroscopic interfacial voids. Bottom-cast bars, which in general are surrounded by better compacted concrete, show a reduction of peak bond strength with increasing corrosion levels.

- The presence of stirrups positively impacts the residual bond strength, and contributes to maintaining bond strength in the presence of corrosion-induced damages in the concrete.
- A decrease in the peak bond strength of the tensile bars in a flexural member, due to yielding, spalling of the concrete or excessive corrosion damages, significantly increases the transmission length between the reinforcement bar and the surrounding concrete, thus changing the primary load-carrying mechanism from beam to arch action. This mechanism decreases as well the remaining available anchorage length.
- A 3-point-bending test is a well-known, symmetrical test set-up, widely used to study the structural behaviour of reinforced concrete beams. However, when testing naturally corroded beams with plain bars, the stress distribution along the reinforcement bars was shown to be strongly asymmetrical at high load levels. Local bond characteristics highly influence the yield penetration length, thus generating asymmetries in the remaining available anchorage length at the end of the bar. In finite element modeling, it is common to utilize symmetries in the structure to minimize computational cost: however, this would have lead to a significant overestimation of the available anchorage length in the presented study.
- Beam and pull-out tests were used in this work to characterize the anchorage and bond-slip behaviour of naturally corroded plain bars. Both test types showed similar trends regarding the influence of corrosion on the bond of plain bars, and gave comparable results in terms of peak and residual bond stresses. Results from pull-out tests, which is an easier and quicker test set-up, can thus likely be used with good confidence to assess the anchorage behaviour of plain bars in structural members.

Q2: Characteristics of corrosion products and surrounding concrete

Multimodal neutron and X-ray computed tomography was selected as a non-destructive method to investigate characteristics and distribution of corrosion products in two

corroded reinforced concrete samples. The samples contained plain bars, one naturally and the other artificially corroded.

- Different factors, deemed important for understanding and modelling the corrosion cracking process, were investigated: the iron-to-rust volume ratio, the thickness of the corrosion products at the steel-concrete interface, and the size and geometrical characteristics of macro-pores. These entities were successfully observed and quantified in the different specimens.
- Differences between the two samples were observed, particularly the distribution of the corrosion products was substantially different between artificial and natural corrosion: in the artificially corroded specimen corrosion products were observed to have diffused through the cement paste, and were in general rather uniformly distributed. In the naturally corroded specimen, corrosion products were instead found in correspondence of macroscopic voids, where large corrosion pits had formed.

Q3: Impact of cracks on corrosion characteristics

The impact of load-induced, transverse cracks on corrosion rate and distribution was studied by composing a dataset of experimental data taken from literature and applying statistical methods to evaluate the correlation between different factors expected to influence the corrosion process. The following was observed:

- No apparent influence of surface crack width on corrosion rate or distribution was observed.
- The distribution of corrosion damages was observed to be influenced by the presence of transversal cracks: corrosion pits were often positioned in the proximity of the cracks, although not all cracks had pits in their influence area. The closer was the pit to a crack, the higher the local corrosion rate of the pit.
- Results point out discrepancies in the type of data collected by different researchers, arguing for the need of clearly defined procedures for the assessment of crack openings and corrosion damage.

6.2 Suggestions for future research

This work focuses on the effects of natural corrosion in existing structures. Parts of this work stress the difference between natural corrosion and corrosion as a result of impressed-current applied to laboratory specimens. The take away of this work,

according to the author, is not, however, that only natural corrosion should be studied. Observation on naturally corroded specimens, and decommissioned structures in general, need to be a bridge between reality and laboratory studies, and used as a basis to create well-defined test specimens able to well capture the actual expected damages for the case of interest. Comparison studies of the structural effects of natural and accelerated corrosion, where specimens corroded with impressed current are designed to mimic damages as observed in natural specimens, may be a further step ahead in this direction.

Based on the work conducted in this thesis, multiple areas of importance for future work were identified:

- *Q1, effect of natural corrosion on bond of plain bars:*

  The conclusions drawn in this study are based on specimens taken from the same decommissioned structure. The type of concrete and the casting technique likely influenced the effect of corrosion damages on the bond strength. Other specimens taken from decommissioned structures should be investigated, with differences in the exposure environment, geometry and, if possible, material properties, to obtain a clear picture of the variation of bond with different factors. Additionally, the presence of stirrups was observed to be an influencing factor on the bond-slip curve: more tests, with changes in stirrup geometry and number of stirrups would help acquire further knowledge, and possibly, calibrate a bond-slip model that takes the effect of stirrups into account.

- *Q2, characteristics of corrosion products and surrounding concrete:*

  This work utilized multimodal neutron and X-ray computed tomography to study the characteristics of corrosion products. However, only two samples, one extracted from Gullspång bridge and the other artificially corroded, were analysed. Corrosion products are expected to change in volume and distribution with the availability of oxygen, as with changes in the current density and the presence of chlorides: different samples, exposed to varying environments, both naturally corroded and corroded with impressed current, should be studied with the same technique, to observe differences and similarities in composition and distribution of the corrosion products. Additionally, multiple scans of the same sample in different stages of the corrosion process could allow for capturing changes in the strain distribution in the sample due to the increasing presence of corrosion products. Such a study could be an important step towards creating a reliable model for the the corrosion cracking process in reinforced concrete structures.

- *Q3, impact of cracks on corrosion characteristics:*

The impact of transversal cracks on corrosion rate and distribution was studied using statistical methods and data collected from literature on experiments conducted on specimens pre-cracked in 3-point bending. A natural second step is to conduct further experiments to collect more data for the dataset. Ideally, these experiments will aim at complementing the collected data, by reducing the correlation seen in the dataset between experimental choices (e.g. choosing high water/binder ratio and small concrete covers). Additionally, variation in surface crack width should include larger values than 0.3 mm, thus exploring the possibility to allow for larger surface crack width when designing structures, based on the chosen concrete cover and water/binder ratio. Finally, results from existing structures will add further value to the collected data.

References

[1] J. Austen, *Pride and Prejudice*. New York: Penguin Classics, 2007, Kindle edition.

[2] B. Bell, "Sustainable bridges.," *European Railway Bridge Problems*, vol. D1.3, 2004.

[3] U. M. Angst, M. R. Geiker, M. C. Alonso, R. Polder, O. B. Isgor, B. Elsener, H. Wong, A. Michel, K. Hornbostel, C. Gehlen, R. François, M. Sanchez, M. Criado, H. Sørensen, C. Hansson, R. Pillai, S. Mundra, J. Gulikers, M. Raupach, J. Pacheco, and A. Sagüés, "The effect of the steel–concrete interface on chloride-induced corrosion initiation in concrete: a critical review by RILEM TC 262-SCI," *Materials and Structures/Materiaux et Constructions*, vol. 52, no. 4, 2019.

[4] A. Jamali, U. Angst, B. Adey, and B. Elsener, "Modeling of corrosion-induced concrete cover cracking: A critical analysis," *Construction and Building Materials*, vol. 42, pp. 225–237, 2013.

[5] K. Tuutti, "Corrosion of steel in concrete," Swedish Cement and Concrete Research Institute, Stockholm, Tech. Rep., 1982.

[6] K. Lundgren, "Effect of corrosion on the bond between steel and concrete: an overview," *Magazine of Concrete Research*, vol. 59, no. 6, pp. 447–461, 2007.

[7] M. Tahershamsi, K. Zandi, K. Lundgren, and M. Plos, "Anchorage of naturally corroded bars in reinforced concrete structures," *Magazine of Concrete Research*, vol. 66, no. 14, pp. 729–744, 2014.

[8] E. Chen, C. G. Berrocal, I. Löfgren, and K. Lundgren, "Correlation between concrete cracks and corrosion characteristics of steel reinforcement in pre-cracked plain and fibre-reinforced concrete beams," *Materials and Structures/Materiaux et Constructions*, vol. 53, no. 2, 2020.

[9] I. Fernandez and C. G. Berrocal, "Mechanical Properties of 30 Year-Old Naturally Corroded Steel Reinforcing Bars," *International Journal of Concrete Structures and Materials*, vol. 13, no. 1, 2019.

[10] R. François, I. Khan, and V. H. Dang, "Impact of corrosion on mechanical properties of steel embedded in 27-year-old corroded reinforced concrete beams," *Materials and Structures/Materiaux et Constructions*, vol. 46, no. 6, pp. 899–910, 2013.

[11] I. Fernandez, M. F. Herrador, A. R. Marí, and J. M. Bairán, "Ultimate Capacity of Corroded Statically Indeterminate Reinforced Concrete Members," *International Journal of Concrete Structures and Materials*, vol. 12, no. 1, Dec. 2018.

[12] M. M. Kioumarsi, M. A. N. Hendriks, J. Kohler, and M. R. Geiker, "The effect of interference of corrosion pits on the failure probability of a reinforced concrete beam," *Engineering Structures*, vol. 114, pp. 113–121, 2016.

[13] L. Bertolini, B. Elsener, P. Pedeferri, and R. Polder, *Corrosion of steel in Concrete. Prevention, Diagnosis, Repair.* Weinheiim, Germany, 2004, p. 392.

[14] S. M and C. LA, "Effect of corrosion rate on the bond strength of corroded reinforcement," *Proceedings of International Conference on Corrosion and Corrosion Protection ofSteel in Concrete*, pp. 591–602, 1994.

[15] S. Robuschi, A. Tengattini, J. Dijkstra, I. Fernandez, and K. Lundgren, "A closer look at corrosion of steel reinforcement bars in concrete using 3D neutron and X-ray computed tomography," *Cement and Concrete Research*, vol. 144, no. March, p. 106 439, 2021.

[16] U. M. Angst, "Predicting the time to corrosion initiation in reinforced concrete structures exposed to chlorides," *Cement and Concrete Research*, vol. 115, no. March 2018, pp. 559–567, 2019.

[17] L. Tolstoy and R. Pevear, *Anna Karenina*. New York: Penguin Classics, 2013, Penguin Clothbound Classics.

[18] C. Andrade, "Some historical notes on the research in corrosion of reinforcement," *Hormigón y Acero*, vol. 69, pp. 21–28, 2018.

[19] A. W. Beeby, "Prediction of Crack Widths in Hardened Concrete.," *Structural Engineer*, vol. 57 A, no. 1, pp. 9–17, 1979.

[20] H. H. Haynes, A. L. Abolitz, A. R. Anderson, I. Boaz, A. D. Boyd, W. J. Cichanski, J. Clarke, J. A. Dobrowolski, J. M. Duncan, R. W. Litton, A. H. Mattock, K. H. Runge, C. E. Smith, R. J. Smith, S. G. Stiansen, A. A. Yee, and T. H. Monnier, "Guide for the Design and Construction of Fixed Offshore Concrete Structures," vol. 75, no. 12, 1978.

[21] D. W. Hobbs, "Concrete deterioration: causes, diagnosis, and minimising risk," *International Materials Reviews*, vol. 46, no. 3, pp. 117–144, 2001.

[22] C.L. Page and K. W. J. Treadaway, "Aspects of electrochemistry of steel in concrete," *Nature*, vol. 5862, no. May, pp. 109–115, 1982.

[23] A. K*ü*ter, "Management of Reinforcement Corrosion," Ph.D. dissertation, DTU, 2009, p. 354.

[24] M. Pourbaix, *Lectures on Electrochemical Corrosion*. Boston, MA: Springer US, 1973.

[25] J. Cairns and S. Millard, "Reinforcement corrosion and its effect on residual strength of concrete structures," English, 1999, 12pp.

[26] U. Angst, F. Moro, M. Geiker, S. Kessler, H. Beushausen, C. Andrade, J. Lahdensivu, A. Köliö, K. I. Imamoto, S. von Greve-Dierfeld, and M. Serdar, "Corrosion of steel in carbonated concrete: Mechanisms, practical experience, and research priorities – A critical review by RILEM TC 281-CCC," *RILEM Technical Letters*, vol. 5, pp. 85–100, 2020.

[27] E. Bastidas-Arteaga, F. Schoefs, M. G. Stewart, and X. Wang, "Influence of global warming on durability of corroding RC structures: A probabilistic approach," *Engineering Structures*, vol. 51, pp. 259–266, 2013.

[28] I. S. Yoon, O. Çopuroğlu, and K. B. Park, "Effect of global climatic change on carbonation progress of concrete," *Atmospheric Environment*, vol. 41, no. 34, pp. 7274–7285, 2007.

[29] B. Šavija and E. Schlangen, "Autogeneous healing and chloride ingress in cracked concrete," *Heron*, vol. 61, no. 1, pp. 15–32, 2016.

[30] U. Angst, B. Elsener, C. K. Larsen, and Ø. Vennesland, "Critical chloride content in reinforced concrete - A review," *Cement and Concrete Research*, vol. 39, no. 12, pp. 1122–1138, 2009.

[31] J. Pacheco and R. B. Polder, "Critical chloride concentrations in reinforced concrete specimens with ordinary Portland and blast furnace slag cement," *Heron*, vol. 61, no. 2, pp. 99–119, 2016.

[32] Y. Cao, C. Gehlen, U. Angst, L. Wang, Z. Wang, and Y. Yao, "Critical chloride content in reinforced concrete — An updated review considering Chinese experience," *Cement and Concrete Research*, vol. 117, no. May 2018, pp. 58–68, 2019.

[33] C. Boschmann Käthler, U. M. Angst, A. M. Aguilar, and B. Elsener, "A novel approach to systematically collect critical chloride contents in concrete in an open access data base," *Data in Brief*, vol. 27, 2019.

[34] C. Chalhoub, R. François, and M. Carcasses, "Critical chloride threshold values as a function of cement type and steel surface condition," *Cement and Concrete Research*, vol. 134, no. February, 2020.

[35] C. Boschmann Käthler, S. L. Poulsen, H. E. Sørensen, and U. M. Angst, "Investigations of accelerated methods for determination of chloride threshold values for reinforcement corrosion in concrete," *Sustainable and Resilient Infrastructure*, vol. 00, no. 00, pp. 1–12, 2021.

[36] D. Boubitsas and L. Tang, "The influence of reinforcement steel surface condition on initiation of chloride induced corrosion," *Materials and Structures/Materiaux et Constructions*, vol. 48, no. 8, pp. 2641–2658, 2015.

[37] U. M. Angst, B. Elsener, C. K. Larsen, and Ø. Vennesland, "Chloride induced reinforcement corrosion: Electrochemical monitoring of initiation stage and chloride threshold values," *Corrosion Science*, vol. 53, no. 4, pp. 1451–1464, 2011.

[38] M. R. Geiker, M. A. Hendriks, and B. Elsener, "Durability-based design: the European perspective," *Sustainable and Resilient Infrastructure*, vol. 00, no. 00, pp. 1–16, 2021.

[39] A. Michel, H. E. Sørensen, and M. R. Geiker, "5 Years of in Situ Reinforcement Corrosion Monitoring in the Splash and Submerged Zone of a Cracked Concrete Element," *Construction and Building Materials*, vol. 285, 2021.

[40] K. Hornbostel, U. M. Angst, B. Elsener, C. K. Larsen, and M. R. Geiker, "Influence of mortar resistivity on the rate-limiting step of chloride-induced macro-cell corrosion of reinforcing steel," *Corrosion Science*, vol. 110, pp. 46–56, 2016.

[41] D. R. Lide, *CRC handbook of chemistry and physics.* Internet Version. Boca Raton, FL, 2005, p. 4368.

[42] K. K. Sagoe-Crentsil and F. P. Glasser, ""Green rust", iron solubility and the role of chloride in the corrosion of steel at high pH," *Cement and Concrete Research*, vol. 23, no. 4, pp. 785–791, 1993.

[43] H. S. Wong, Y. X. Zhao, A. R. Karimi, N. R. Buenfeld, and W. L. Jin, "On the penetration of corrosion products from reinforcing steel into concrete due to chloride-induced corrosion," *Corrosion Science*, vol. 52, no. 7, pp. 2469–2480, 2010.

[44] Q. F. Liu, R. K. L. Su, and F. Xu, "Quantification of the actual expansion and deposition of rust in reinforced concrete," *Construction and Building Materials*, vol. 297, p. 123 760, 2021.

[45] Y. Yingshu, Yongsheng Ji, and Surendra P. Shah, "Comparison of Two Accelerated Corrosion Techniques for Concrete Structures," *ACI Structural Journal*, vol. 104, no. 3, pp. 344–347, 2007.

[46] S. Williamson and L. A. Clark, "Effect of corrosion and Load on Reinforcement Bond Strength," *Structural Engineering International: Journal of the International Association for Bridge and Structural Engineering (IABSE)*, pp. 113–119, 2002, ISSN: 00917613.

[47] G. Malumbela, P. Moyo, and M. Alexander, "A step towards standardising accelerated corrosion tests on laboratory reinforced concrete specimens," *Journal of the South African Institution of Civil Engineering*, vol. 54, no. 2, pp. 78–85, 2012, ISSN: 10212019.

[48] S. A. Austin, R. Lyons, and M. J. Ing, "Electrochemical behavior of steel-reinforced concrete during accelerated corrosion testing," *Corrosion*, vol. 60, no. 2, pp. 203–212, 2004, ISSN: 00109312.

[49] W. Zhang, R. François, R. Wang, Y. Cai, and L. Yu, "Corrosion behavior of stirrups in corroded concrete beams exposed to chloride environment under sustained loading," *Construction and Building Materials*, vol. 274, 2021.

[50] E. Chen, C. G. Berrocal, I. Fernandez, I. Löfgren, and K. Lundgren, "Assessment of the mechanical behaviour of reinforcement bars with localised pitting corrosion by Digital Image Correlation," *Engineering Structures*, vol. 219, no. June, p. 110 936, 2020, ISSN: 18737323.

[51] D. V. Val and L. Chernin, "Serviceability Reliability of Reinforced Concrete Beams with Corroded Reinforcement," *Journal of Structural Engineering*, vol. 135, no. 8, pp. 896–905, 2009, ISSN: 0733-9445.

[52] Y. Du, M. Cullen, and C. Li, "Structural effects of simultaneous loading and reinforcement corrosion on performance of concrete beams," *Construction and Building Materials*, vol. 39, pp. 148–152, 2013, ISSN: 09500618.

[53] D. Coronelli and P. Gambarova, "Structural Assessment of Corroded Reinforced Concrete Beams: Modeling Guidelines," *Journal of Structural Engineering*, vol. 130, no. 8, pp. 1214–1224, 2004.

[54] V. H. Dang and R. François, "Influence of long-term corrosion in chloride environment on mechanical behaviour of RC beam," *Engineering Structures*, 2013, ISSN: 01410296.

[55] C. Naito, R. Sause, I. Hodgson, S. Pessiki, and T. Macioce, "Forensic Examination of a Noncomposite Adjacent Precast Prestressed Concrete Box Beam Bridge," *Journal of Bridge Engineering*, vol. 15, no. 4, pp. 408–418, 2010, ISSN: 1084-0702.

[56] M. Tahershamsi, "Structural Effects of Reinforcement Corrosion in Concrete Structures," Ph.D. dissertation, Chalmers University of Technology, 2016, ISBN: 9789173855525.

[57] CEB-FIP Bulletin n.10, "Bond of reinforcement in concrete: State of the art," *FIB Bulletin 10*, no. December, p. 434, 2000.

[58] J. Cairns, Y. Du, and D. Law, "Influence of corrosion on the friction characteristics of the steel/concrete interface," *Construction and Building Materials*, vol. 21, no. 1, pp. 190–197, 2007.

[59] ——, "Structural performance of corrosion-damaged concrete beams," *Magazine of Concrete Research*, vol. 60, no. 5, pp. 359–370, 2008.

[60] A. A. Almusallam, A. S. Al-Gahtani, A. R. Aziz, and Rasheeduzzafar, "Effect of reinforcement corrosion on bond strength," *Construction and Building Materials*, vol. 10, no. 2, pp. 123–129, 1996.

[61] Y. Auyeung, P. Balaguru, and L. Chung, "Bond behavior of corroded reinforcement bars," *ACI Structural Journal*, vol. 97, no. 2, pp. 214–220, 2000.

[62] M. Blomfors, K. Zandi, K. Lundgren, and D. Coronelli, "Engineering bond model for corroded reinforcement," *Engineering Structures*, vol. 156, no. December 2017, pp. 394–410, 2018.

[63] G. M. Verderame, P. Ricci, M. Esposito, and F. C. Sansiviero, "Le Caratteristiche Meccaniche degli Acciai Impiegati nelle Strutture in c.a. realizzate dal 1950 al 1980," *XXVI Convegno Nazionale AICAP*, 2011.

[64] D. Abrams, "Test of Bond Between Concrete and Steel," Ph.D. dissertation, 1913.

[65] ACI Committee 408, "ACI 408R-03 Bond and Development of Straight Reinforcing Bars in Tension," *American Concrete Institute*, pp. 1–49, 2003.

[66] J. Cairns, Y. Du, and D. Law, "Residual bond strength of corroded plain round bars," *ConRes*, vol. 58, no. 4, pp. 221–231, 2006, ISSN: 00249831.

[67] FIB, *fib Model Code*, September. 2013, pp. 152–189.

[68] G. M. Verderame, P. Ricci, G. D. Carlo, and G. Manfredi, "Cyclic bond behaviour of plain bars. Part I: Experimental investigation," *Construction and Building Materials*, vol. 23, no. 12, pp. 3499–3511, 2009, ISSN: 09500618.

[69] G. M. Verderame, G. De Carlo, P. Ricci, and G. Fabbrocino, "Cyclic bond behaviour of plain bars. Part II: Analytical investigation," *Construction and Building Materials*, vol. 23, no. 12, pp. 3512–3522, 2009, ISSN: 09500618.

[70] J. Melo, T. Rossetto, and H. Varum, "Experimental study of bond–slip in RC structural elements with plain bars," *Materials and Structures/Materiaux et Constructions*, vol. 48, no. 8, pp. 2367–2381, 2015, ISSN: 13595997.

[71] L. R. Feldman and F. M. Bartlett, "Bond strength variability in pullout specimens with plain reinforcement," *ACI Structural Journal*, vol. 102, no. 6, pp. 860–867, 2005, ISSN: 08893241.

[72] J. Cairns and L. Feldman, "Strength of laps and anchorages of plain surface bars," no. November 2017, pp. 1782–1791, 2018.

[73] R. Gustavson, "Experimental studies of the bond response of three-wire strands and some influencing parameters," *Materials and Structures/Materiaux et Constructions*, vol. 37, no. 266, pp. 96–106, 2004, ISSN: 13595997.

[74] K. Lundgren and J. Magnusson, "Three-Dimensional Modeling of Anchorage Zones in Reinforced Concrete," *Journal of Engineering Mechanics*, vol. 127, no. 7, pp. 693–699, 2001.

[75] H. Nasser, C. Van Steen, L. Vandewalle, and E. Verstrynge, "An experimental assessment of corrosion damage and bending capacity reduction of singly reinforced concrete beams subjected to accelerated corrosion," *Construction and Building Materials*, vol. 286, p. 122 773, 2021.

[76] W. Dong, J. Ye, Y. Murakami, H. Oshita, S. Suzuki, and T. Tsutsumi, "Residual load capacity of corroded reinforced concrete beam undergoing bond failure," *Engineering Structures*, vol. 127, pp. 159–171, 2016.

[77] L. R. Feldman and F. M. Bartlett, "Bond in flexural members with plain steel reinforcement," *ACI Structural Journal*, vol. 105, no. 5, pp. 552–560, 2008, ISSN: 08893241.

[78] W. Zhang, R. François, and L. Yu, "Influence of load-induced cracks coupled or not with top-casting-induced defects on the corrosion of the longitudinal tensile reinforcement of naturally corroded beams exposed to chloride environment under sustained loading," *Cement and Concrete Research*, vol. 129, no. October 2019, p. 105 972, 2020.

[79] W. Zhang, R. François, Y. Cai, J. P. Charron, and L. Yu, "Influence of artificial cracks and interfacial defects on the corrosion behavior of steel in concrete during corrosion initiation under a chloride environment," *Construction and Building Materials*, vol. 253, p. 119 165, 2020.

[80] E. Rossi, R. Polder, O. Copuroglu, T. Nijland, and B. Šavija, "The influence of defects at the steel/concrete interface for chloride-induced pitting corrosion of naturally-deteriorated 20-years-old specimens studied through X-ray Computed Tomography," *Construction and Building Materials*, vol. 235, p. 117 474, 2020.

[81] Y. Cai, W. Zhang, L. Yu, M. Chen, C. Yang, R. François, and K. Yang, "Characteristics of the steel-concrete interface and their effect on the corrosion of steel bars in concrete," *Construction and Building Materials*, vol. 253, p. 119 162, 2020.

[82] R. Palsson and M. S. Mirza, "Mechanical response of corroded steel reinforcement of abandoned concrete bridge," *ACI Structural Journal*, vol. 99, no. 2, pp. 157–162, 2002.

[83] C. G. Berrocal, I. Löfgren, and K. Lundgren, "The effect of fibres on steel bar corrosion and flexural behaviour of corroded RC beams," *Engineering Structures*, vol. 163, no. February, pp. 409–425, 2018.

[84] V. H. Dang and R. François, "Prediction of ductility factor of corroded reinforced concrete beams exposed to long term aging in chloride environment," *Cement and Concrete Composites*, vol. 53, pp. 136–147, 2014.

[85] M. G. Stewart, "Mechanical behaviour of pitting corrosion of flexural and shear reinforcement and its effect on structural reliability of corroding RC beams," *Structural Safety*, vol. 31, no. 1, pp. 19–30, 2009.

[86] A. Boschmann Kathler, U. Angst, M. Wagner, C. Larsen, and B. Elsener, "Effect of cracks on chloride- induced corrosion of steel in concrete - a review," no. September, p. 41, 2017.

[87] CEN, *EN 1992-1-1:2004: E.* 2004, ISBN: 91.010.30; 91.080.40.

[88] C. B. Käthler, U. M. Angst, K. Hornbostel, and B. Elsener, "Critical analysis of experiments on reinforcing bar corrosion in cracked concrete," *ACI Materials Journal*, vol. 117, no. 3, pp. 145–154, 2020.

[89] A. Beeby, *Concrete in the oceans; cracking and corrosion.* Wexham Springs.: CIRIA/UEG et al., 1978, p. 77.

[90] K. Tammo and S. Thelandersson, "Crack opening near reinforcement bars in concrete structures," *Structural Concrete*, vol. 7, no. 4, pp. 137–143, 2006.

[91] L. Yu, R. François, V. H. Dang, V. L'Hostis, and R. Gagné, "Development of chloride-induced corrosion in pre-cracked RC beams under sustained loading: Effect of load-induced cracks, concrete cover, and exposure conditions," *Cement and Concrete Research*, vol. 67, pp. 246–258, 2015.

[92] M. Otieno, H. Beushausen, and M. Alexander, "Towards incorporating the influence of cover cracking on steel corrosion in RC design codes: The concept of performance-based crack width limits," *Materials and Structures/Materiaux et Constructions*, vol. 45, no. 12, pp. 1805–1816, 2012.

[93] A. Blagojevic, *The Influence of Cracks on the Durability and Service Life of Reinforced Concrete Structures in relation to Chloride-Induced Corrosion.* 2016, p. 215.

[94] M. Geiker, T. Danner, A. Michel, A. Belda Revert, O. Linderoth, and K. Hornbostel, "25 Years of Field Exposure of Pre-Cracked Concrete Beams; Combined Impact of Spacers and Cracks on Reinforcement Corrosion," *Construction and Building Materials*, vol. 286, no. March, 2021.

[95] M. B. Otieno, M. G. Alexander, and H. D. Beushausen, "Corrosion in cracked and uncracked concrete - influence of crack width, concrete quality and crack reopening," *Magazine of Concrete Research*, vol. 62, no. 6, pp. 393–404, 2010.

[96] P. Schießl and M. Raupach, "Laboratory studies and calculations on the influence of crack width on chloride-induced corrosion of steel in concrete," *ACI Materials Journal*, vol. 94, no. 1, pp. 56–62, 1997.

[97] O. Stamati, E. Roubin, E. Andò, and Y. Malecot, "Phase segmentation of concrete x-ray tomographic images at meso-scale: Validation with neutron tomography," *Cement and Concrete Composites*, vol. 88, pp. 8–16, 2018.

[98] E. Roubin, E. Andò, and S. Roux, "The colours of concrete as seen by X-rays and neutrons," *Cement and Concrete Composites*, vol. 104, no. December 2018, p. 103 336, 2019.

[99] D. Dauti, A. Tengattini, S. Dal Pont, N. Toropovs, M. Briffaut, and B. Weber, "Analysis of moisture migration in concrete at high temperature through in-situ neutron tomography," *Cement and Concrete Research*, vol. 111, no. February, pp. 41–55, 2018.

[100] D. Dauti, A. Tengattini, S. D. Pont, N. Toropovs, M. Briffaut, and B. Weber, "Some Observations on Testing Conditions of High-Temperature Experiments on Concrete: An Insight from Neutron Tomography," *Transport in Porous Media*, no. 0123456789, 2020.

[101] P. Zhang, Z. Liu, Y. Wang, J. Yang, S. Han, and T. Zhao, "3D neutron tomography of steel reinforcement corrosion in cement-based composites," *Construction and Building Materials*, vol. 162, no. December 2017, pp. 561–565, 2018.

[102] B. Šavija, M. Luković, S. A. S. Hosseini, J. Pacheco, and E. Schlangen, "Corrosion induced cover cracking studied by X-ray computed tomography, nanoindentation, and energy dispersive X-ray spectrometry (EDS)," *Materials and Structures/Materiaux et Constructions*, vol. 48, no. 7, pp. 2043–2062, 2015.

[103] L. Calabrese and E. Proverbio, "A Review on the Applications of Acoustic Emission Technique in the Study of Stress Corrosion Cracking," *Corrosion and Materials Degradation*, vol. 2, no. 1, pp. 1–33, 2020.

[104] C. Van Steen, L. Pahlavan, M. Wevers, and E. Verstrynge, "Localisation and characterisation of corrosion damage in reinforced concrete by means of acoustic emission and X-ray computed tomography," *Construction and Building Materials*, vol. 197, pp. 21–29, 2019.

[105] C. Van Steen, E. Verstrynge, M. Wevers, and L. Vandewalle, "Assessing the bond behaviour of corroded smooth and ribbed rebars with acoustic emission monitoring," *Cement and Concrete Research*, vol. 120, no. August 2018, pp. 176–186, 2019.

[106] C. Van Steen, H. Nasser, E. Verstrynge, and M. Wevers, "Acoustic emission source characterisation of chloride-induced corrosion damage in reinforced concrete," *Structural Health Monitoring*, 2021, ISSN: 17413168.

[107] C. Van Steen and E. Verstrynge, "Degradation Monitoring in Reinforced Concrete with 3D Localization of Rebar Corrosion and Related Concrete Cracking," *Applied Sciences*, vol. 11, no. 15, p. 6772, 2021.

[108] D. Adams, *The restaurant at the end of the universe*. New York: Del Rey books, 2005.

[109] TNO, *DIANA Finite Element Analysis*, release 10.2.

[110] J. R. R. Tolkien, *The Hobbit*. Chicago: Harper Collins, 2012.

[111] J. K. Rowling, *Harry Potter and the Deathly Hallows*. Bloomsbury, 2007.

[112] G. Garcia Marquez and E. Grossman, *Love in the time of cholera*. Penguin Classics, 2007.